The University of Manchester

# Alternative High-Power Transmission Technology Using Gas Insulated Transmission line (GIL)

Third Year Individual Project – Final Report

April 2017

**Seunghwan Kim**

9767991

Dr Tony Lujia Chen

School of Electrical and Electronic Engineering

**Abstract**

The necessity of renewable energy has come to the fore as increasing environmental issues require humans to reduce the amount of greenhouse gases resulting in global warming. However, power stations using renewable sources are often at a considerable distance from load centres. The overhead line (OHL) was used for long-distance high voltage transmission lines, but it faces construction difficulties. Thus, underground transmission systems have come into the request. Currently, an alternative transmission system is gas insulated transmission line (GIL). This paper investigates the use of GIL as an alternative transmission system, which can be used when OHL cannot be constructed by being significantly superior to XLPE cable, with regards to power transfer capabilities and lifetime costs.

This report draws a conclusion in both perspectives that power transfer capabilities and lifetime costs by comparing with XLPE cable and OHL with developing simulation models. For simulation, two software were used (PSCAD and Simulink) for line parameter calculations and designing simulation models respectively. The GIL simulation model is utilised to analyse maximum line length (i.e. the capability of power transfer of transmission line for GIL, XLPE cable, and OHL) and to evaluate the GIL in different conditions according to line length, loading condition, and lagging/leading power factor.

The simulation is carried out with a 420 kV GIL model using Simulink for GIL evaluation. To figure out the effect of GIL line length regarding a voltage, current, real power, and reactive power, the GIL simulation model was measured at every 50 km from the sending end up to 500 km. The effect of GIL loading condition and power factor was simulated for both 300 km and 500 km with load conditions, from 0 % to 120 % in every 20 %, and lagging/leading power factors, 0.9, 0.95, 0.99, and unity.

The lifetime costs comparison was studied using wind farms model in the UK. The average capacity factor and operational capacities were set up as 33.6 % and 6,713.52 MW respectively, and the costs per MWh as ￡48.0. The total lifetime costs were calculated by summation using the capital cost for installation, the net present values of the cost of losses and the cost of operation and maintenance.

# Contents

# 1. Introduction

## 1.1. Motivation

The fast-economic growth, improvement of quality in national life and progress of renewable energy source gives rise to a necessity for long distance bulk-power transfer. Those issues are already resolved by building technically and an economically outstanding overhead lines (OHL), which are already widely used in long-distance bulk power transfer. However, the overhead connection is having difficulties in securing adequate land to be constructed in more extensive metropolitan areas at the present-day. The troubles have become more critical because of new town development, landscape impediment, and electromagnetic waves by which undergrounding transmission line is now inevitable. An alternative is gas insulated transmission lines (GIL) which is developed for bulk-power transmission line over long distance especially as undergrounding transmission system. GIL is an alternative way to get over the environmental problems of OHL with GIL's environmental advantages [1] as follows, detailed in the literature review in section 2.1.

- High reliability and long operational lifetime
- Low electromagnetic field
- High level of personal safety

Due to the reasons, GIL is much more suitable in the social environment in the present and future. With GIL's environmental strength, the further comparison of the different views must be demonstrated between transmission lines of its electrical capability for long distance high-power transfer, as well as economic aspect cannot be overlooked.

## 1.2. Aims and Objectives

This project aims to evaluate the GIL concerning its electrical capability and lifetime costs by comparison to XLPE cable and OHL using PSCAD and Simulink.

The objectives are:

- Computing line constant of the GIL, XLPE cable and OHL using PSCAD
- Estimating maximum line length of the GIL using Simulink

- Comparing the maximum line length with XLPE cable and OHL
- Evaluating GIL technology in different conditions using Simulink
- Computing lifetime costs of GIL, XLPE cable, and OHL
- Comparing the lifetime costs between transmission technologies
- Comprehensive evaluation

The approach to evaluating the GIL in this project is indicated in figure 1 by a flow chart.

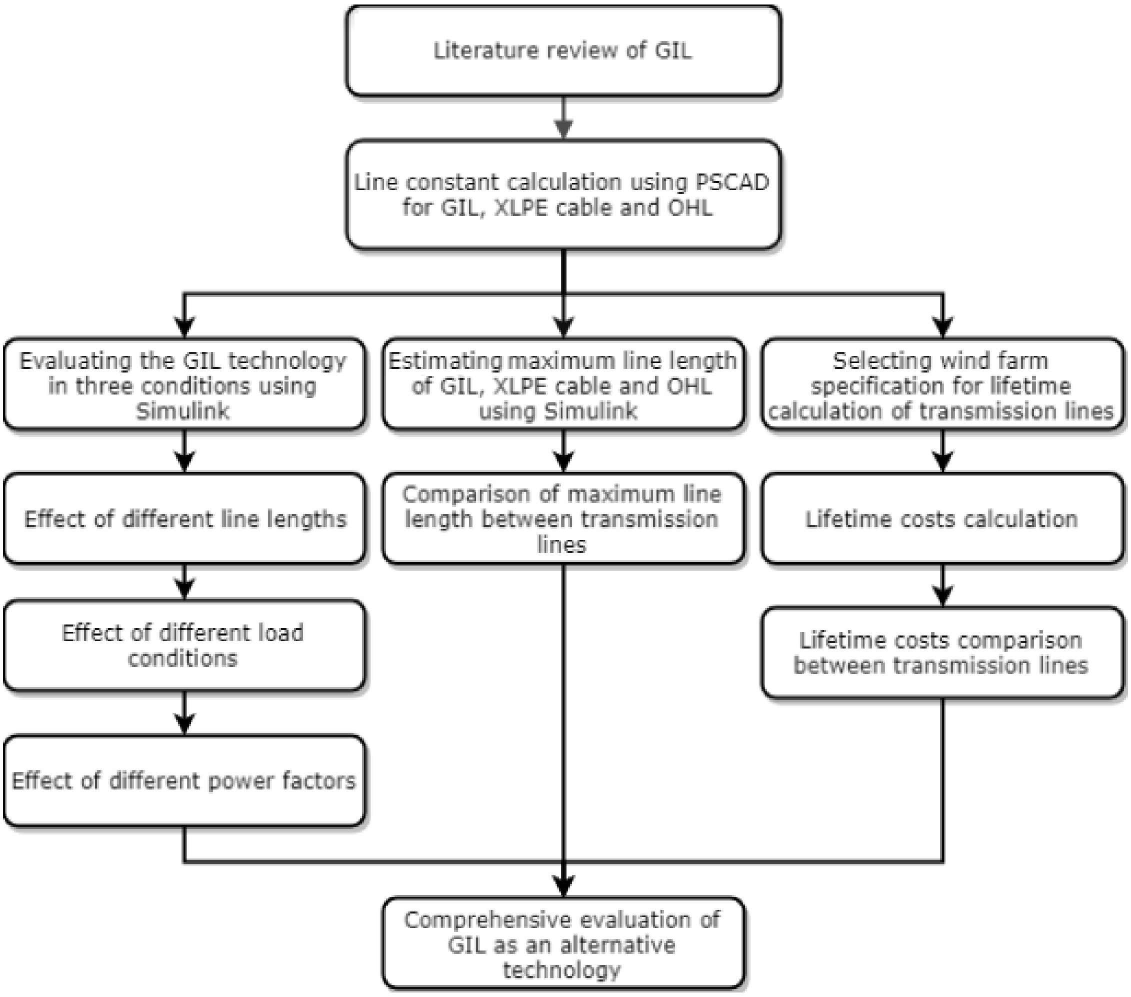


Figure 1 Flow Diagram of Approaches toward Comprehensive Evaluation of GIL

## 2. Literature review

### 2.1. GIL Transmission Line Overview

The GIL can be applied in various voltage levels of transmission from the range of 135kV up to 1200kV [1,5] and the application having high power capacity up to 3000MW at 420/550 kV [1] is a global trend at which economic optimisation is feasible. GIL has its characteristics of high voltage capacity that equals to the overhead line [1]. For main technical data of the GIL in the 2nd generation, its typical rated current is over 4000A and rated short-circuit current is 63kA/3s at 420kV nominal voltage level [3]. The tube-shaped conductor for power transmission is made by aluminium with big cross-section area to achieve low electrical resistance, and the resistance is also related to the geometric dimension of the GIL(i.e. the line parameters depend on the size of the conductor, gas insulation and enclosure of pipe). The pipe diameter and wall thickness are generally around 500mm and 10mm for 420kV/550kV for the current transported smoothly [1]. The length of conductor is decided by conditions on-site but produced by the distance from 12m to 18m in general [1].

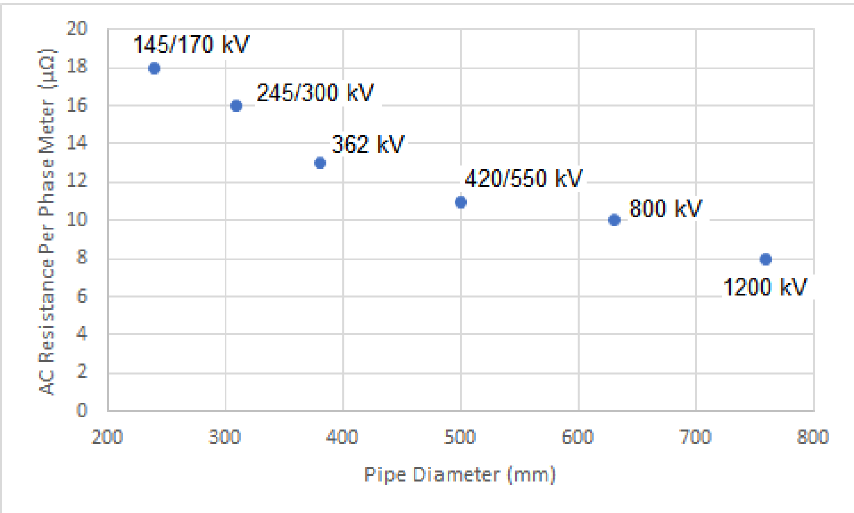


Figure 2 Typical value of resistance by GIL size [1]

The GIL can be constructed in diverse mechanical design such as above-ground installation, tunnel installation, direct burial or vertical installation, so it is possible for the operator to take a flexible action regarding environmental or geometrical condition.

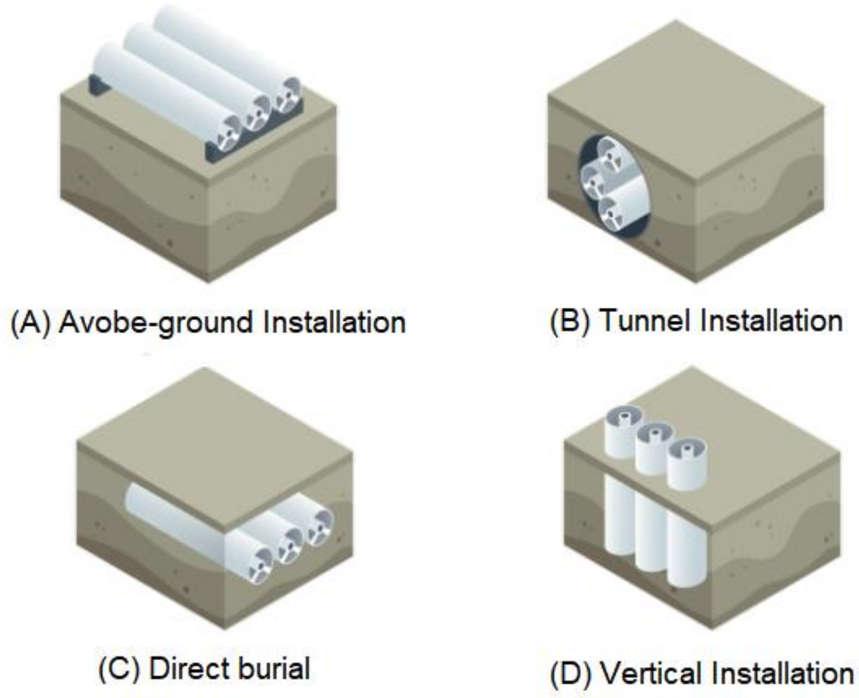


Figure 3 Versatility in laying methods, Siemens AG [4]

The GIL is composed of gas-filled insulators, support insulators, aluminium enclosure, and conductor. The pipe-shaped aluminium conductor is placed at the centre sustained by support insulators made of epoxy resin. By the structure of the GIL of conductor wrapped by aluminium enclosure, it is less sensitive to external factors than overhead line and has optically advantage since it is typically buried. With GIL's solid structure, the reliability of GIL technology for operation has been proven for 44 years without any failures (the first GIL was constructed in 1974) [1].

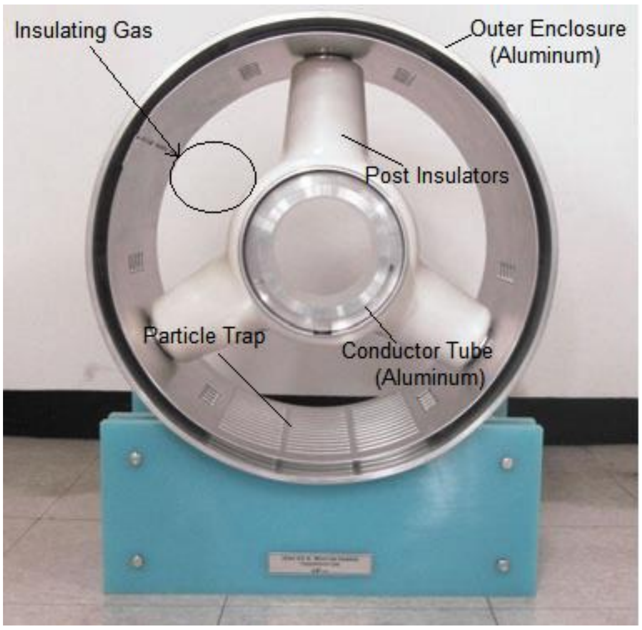


Figure 4 Cross-sectional Structure of GIL

The main drawback of GIL tech is the use of SF6 gas due to its very high environmental impact since the pure SF6 gas was used in the first generation. However, the gas mixture in the second generation uses N2 for main insulating gas and SF6 for ancillary gas. This reduces worries of greenhouse gas exhaustion.

Additionally, there are few environmental advantages of the GIL. The GIL is typically constructed under the ground in various methods such as in-tunnel, trench-laid, or directly buried [1]. This gives GIL non-visible advantage to the public, as well as less noisy by corona [1], in contrast with OHL shown in figure 3 – (b, c). The GIL also emits less electromagnetic field than XLPE cable and OHL [1] shown in figure 5.

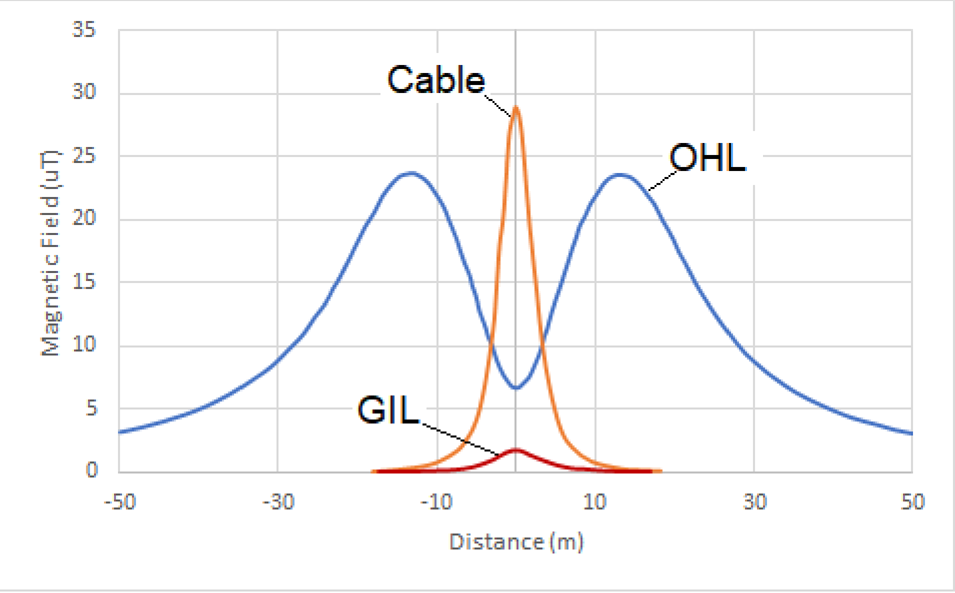


Figure 5 Magnetic flux density comparison for GIL, cable, and OHL [1]

## 2.2. GIL Line Constant Calculation

The single-phase model of a GIL at the positive sequence as can be seen in figure 6 is an approximation to compute GIL line constant when solid-bonded for the enclosures of the GIL since the circulation of induced currents is almost constant over the enclosures [7] in terms of magnitude and opposite to the phase current in angle [6]. This is allowed by very low resistive of the outer enclosure. Thus, the line calculation of the GIL can be derived from the positive sequence circuit and which is computable according to the coaxial configurations.

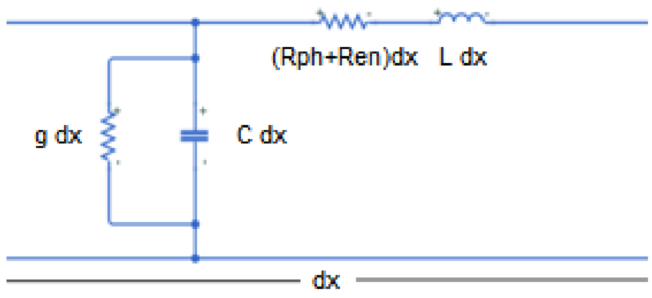


Figure 6 The Positive Sequence Single Phase model for GIL

Where $R_{ph}$ is the resistance of the phase conductor, $R_{en}$ is the resistance of the enclosure, L is inductance of the circuit, C is the capacitance of the circuit, and g is conductance of the circuit

- **GIL resistance "R"**

The resistance R per unit length must be equal to the sum of the resistance $R_{ph}$ and $R_{en}$ [6] since the total losses is fixed per unit length in the model figure 6

$R_{total} = R_{ph} + R_{en}$ [Ω/km] ………………………………………………………………(1)

The skin effects and proximity effects are negligible [8] for $R_{ph}$ and $R_{en}$ to be evaluated as DC resistance calculation. The value of the resistance $R_{ph}$ is calculated by:

$R_{ph}=\frac{\rho_{ph}}{S_{ph}}$ [Ω/km]……………………………………………………………………………(2)

Where $\rho_{ph}$ is resistivity of the phase conductor [$\Omega \mathrm{mm}^2$/km] and $S_{ph}$ = cross-sectional area of the phase conductor,$\pi({R_2}^2 - {R_1}^2)$ $[\mathrm{mm}^2]$

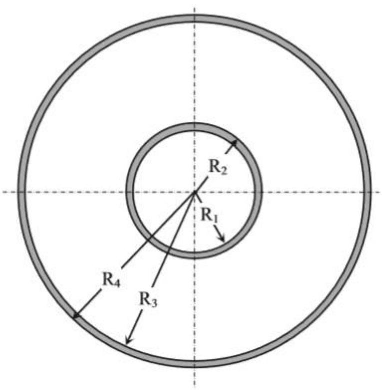


Figure 7 Cross-sectional structure of GIL

Analogously, the value of the resistance $R_{en}$ can be calculated by:

$$R_{en}=\frac{\rho_{en}}{S_{en}}\ [\Omega \mathrm{km}^{-1}] \quad (3)$$

Where $\rho_{en}$ is resistivity of the enclosure $[\Omega \mathrm{mm}^2 \mathrm{km}^{-1}]$ and $S_{en}$ is cross-sectional area of the enclosure, $\pi({R_4}^2 - {R_3}^2)$ $[\mathrm{mm}^2]$

- **GIL inductance "L"**

By considering the structure of GIL from Figure 7 as typical coaxial cable with the solid bonded enclosure, the magnitude of opposite currents flowing are uniformly distributed over the enclosure without skin and proximity effects [7]. The inductance per unit length can be calculated by:

$$L_{total} = L_{ph} + L_{mf} + L_{en} \quad (4)$$

Where $L_{ph}$ is internal inductance of phase conductor, $L_{mf}$ is inductance by a magnetic field between a phase conductor and magnetic field and $L_{en}$ is enclosure internal inductance

The value of $L_{mf}$ can be calculated simply by integrating the magnetic field between $R_2$ and $R_3$ from the Figure 7, with the assumed hypothesis that the magnetic field between enclosure and external is zeroed [7].

$$L_{mf} = \frac{\mu_0}{2\pi} ln\frac{R_3}{R_2}\ [\mathrm{Hm}^{-1}] \quad (5)$$

Where $\mu_0$ is the magnetic permeability of the free space ( $4\pi \times 10^{-7}\ \mathrm{Hm}^{-1}$)

To achieve the optimisation in the configuration of the electric field, $ln\frac{R_3}{R_2}$ is very close to 1 in current installations. The inductance for both $L_{ph}$ and $L_{en}$ can be expressed by the formulae (6) and (7) [7].

$$L_{ph} = \frac{\mu_0}{2\pi}\left[\frac{{R_1}^4}{({R_2}^2-{R_1}^2)^2} ln\left(\frac{R_2}{R_1}\right) + \frac{({R_2}^2-3{R_1}^2)}{4({R_2}^2-{R_1}^2)}\right]\ [\mathrm{Hm}^{-1}] \quad (6)$$

$$L_{en} = \frac{\mu_0}{2\pi}\left[\frac{{R_4}^4}{({R_4}^2-{R_3}^2)^2} ln\left(\frac{R_4}{R_3}\right) + \frac{({R_3}^2-3{R_4}^2)}{4({R_4}^2-{R_3}^2)}\right]\ [\mathrm{Hm}^{-1}] \quad (7)$$

- **GIL capacitance "C"**

The value of GIL capacitance per unit length can be calculated easily by considering the cylindrical symmetry [2] with the permittivity of the insulating gas mixture as for the free space, $\varepsilon_0 = 8.8542\ \times 10^{-12}\ [\mathrm{Fm}^{-1}]$.

$$C = \frac{2\pi\varepsilon_0}{ln\frac{R_3}{R_2}}\ [\mathrm{Fm}^{-1}] \ \rightarrow \ C = \frac{1}{18ln\frac{R_3}{R_2}}[\mu\mathrm{Fm}^{-1}] \qquad (8)$$

- **GIL Shunt conductance “g”**

The N2 and SF2 gas mixture used for insulation matter has significantly small loss factor that causes the negligible result when compared to the small Joule longitudinal losses [7] since low resistance R, and it is always estimated that g = 0 in economic evaluations.

## 2.3. Limitation of Power Flow

The electrical limitation factor such as the voltage drop limit and stability limit is a critical concept to decide the transmission system for long distance technology [2]. The length of AC transmission line is mainly influenced by electrical capacitance over the line by which charging current increases and this results in a reduction of transmitting real power and a voltage drop at the load.

- **Thermal limits**

The thermal power flow limits are considered since the expansion of phasor conductor and enclosure as well as extra losses for GIL transmission system. The electric current inside conductor heats up the transmission lines. Because of the reason, in simulation, the current flowing over the GIL must be below the thermal limits shown in table 1. When the thermal current limit of the GIL is compared to other transmission systems that are an overhead line, oil cable, and XLPE cable, the GIL tunnel-laid technology has the highest thermal power limit [1].

Table 1 Thermal Power Limits in Different Transmission Lines [1]

| Transmission systems | Type | Thermal power limit (MVA) |
|---|---|---|
| GIL Tunnel-laid | Ø 520mm grounded | 2180 |
| XLPE cable 1600$\mathrm{mm}^2$ Tunnel-laid | Cross-bonded | 1150 |
| Oil cable 1200 $\mathrm{mm}^2$ Tunnel-laid | Cross-bonded | 1120 |
| Overhead line | 4 X 240/40A1/St | 1790 |

- **Voltage drop limits**

With phase shift of power transferred over distance, the magnitude of voltage drops over distance. For the voltage limits for the offshore transmission system, the maximum allowable voltage decrease is limited as between +5% and -10% of the sending end voltage as stated by SQSS, National Electricity Transmission System Security and Quality of Supply Standard [9]. The voltage drops limits decrease as transmission distance and as phase shift increases, but decreased voltage drop limits can be compensated by the inclusion of shunt capacitors at the end of the line, and this is much cheaper than reconstructing the transmission lines.

- **Surge impedance loading limits**

The reactive power is produced on transmission lines because of the natural capacitance within it as well as electrical phase shift occurs as power transferred over the transmission line. As more and more the phase shift rises, the embedded line in the system is getting more unstable under electrical disturbances. Mostly, the power flow must be limited to such an extent as to the Surge Impedance Loading (SIL) of the transmission line. Surge impedance loading can be estimated by the square of the sending end voltage [$V_s$] divided by the characteristic impedance [$Z_0$] in the formula below [10].

$$\mathrm{SIL} = \frac{{V_S}^2}{|Characteristic\ Impedance\ Z_0\ |} \qquad (9)$$

# 3. Transmission Line Modelling

## 3.1. Line Parameter calculation for the GIL, XLPE cable and OHL

- **GIL line parameters.**

The GIL line constants are calculated by building a geometrical structure on the power systems computer-aided design platform (PSCAD) based on the Bergeron model [12].

Bergeron model is a Norton equivalent model that is a travelling wave line model based on travelling wave theory with lumped resistance and a distributed LC parameter [11], and the model is occasionally adopted to build a long-distance power transmission network model, and it represents the elements of inductance and capacitance in distributed means [11]. The lumped resistance is showed in distributed series resistance as half of the resistance in the centre of the line and a quarter of resistance at each end [12]. The model in Figure 8 [11] is built for illustrating divided resistances at centre and each end.

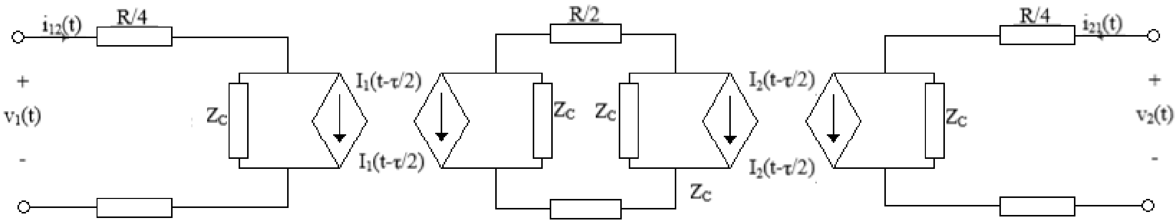


Figure 8 Equivalent Transmission Line Model using Bergeron Model

The circuit in Figure 8 can be collapsed into two parts by splitting the circuit at the centre to calculate the current of the circuit. To divide the circuit, the middle resistance can be divided into two parts of R/4 resistances [12]. With half section of the middle circuit, the cable current can be calculated by voltage division. However, the interest of modelling is to figure out the terminals of the cable model. Two distributed circuit can be cascaded by removing variables at the mid-point with a travelling time of the transmission line $\tau$ shown in the Formulas [11] below.

$$I_1(\mathrm{t}-\tau) = \frac{v_2(t-\tau)}{Z_C+R/4} - \left(\frac{Z_C-R/4}{Z_C+R/4}\right) \cdot I_2(t-\tau) \quad \text{.....(10)}$$

$$I_2(\mathrm{t}-\tau) = \frac{v_1(t-\tau)}{Z_C+R/4} - \left(\frac{Z_C-R/4}{Z_C+R/4}\right) \cdot I_1(t-\tau) \quad \text{.....(11)}$$

The Bergeron cable modelling can be adopted when a specific frequency is considered over whole transmission line because the only fundamental frequency is represented apart from harmonics [12].

The structural characteristic of the GIL is that GIL can be represented by three single cores and each line includes cylindrical sing phase conductor wrapped by the enclosure. Both conductor and enclosure are made of aluminium alloy with its resistivity, $\rho = 2.28 \times 10^{-8}$ Ωm, and relative permeability, $\mu_r = 1$ [1]. Insulated gas mixture is filled in the room between conductor and enclosure with a relative permittivity $\varepsilon_r$ = 1 [1]. External surface of the line (i.e. outer surface of enclosure) can be coated by polyethylene or polypropylene to protect GIL from corrosion [2]. For simulation, polyethylene is assumed to be used by 5mm of thickness with a relative permittivity, $\varepsilon_r$ = 2.25. For the soil resistivity, 100 Ωm is used to represent usual soil resistivity.

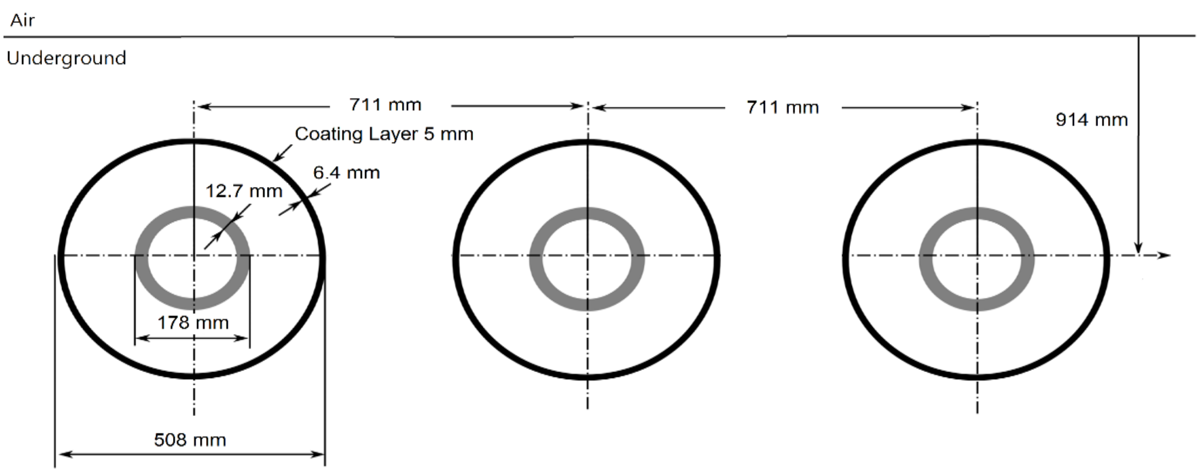


Figure 9 Geometric Dimensions of GIL for simulation using PSCAD

The electrical parameters in Table 2 are acquired by the geometrical characteristics shown in Figure 9 at 50 Hz of steady state frequency by PSCAD line constant program. Table 2 shows both calculated results and simulated results. Calculated results are computed by hand with mathematical process introduced in chapter 2.2. Also, series impedance matrix (Z) and admittance matrix (Y) are generated. When both results are compared, the results show a slight difference, but it is relatively small apart from resistance and surge impedance loading (SIL).

Table 2 Simulated Line Constants for GIL

| Electrical parameters (per phase) | | Units | Calculated results | Simulated results |
|---|---|---|---|---|
| Resistance | r | mΩ/km | 7.0971 | 7.56 |
| Inductance | l | mH/km | 0.2158 | 0.2159 |
| Capacitance | C | uF/km | 0.0543 | 0.05437 |
| Conductance | g | nS/km | negligible | negligible |
| Characteristic Impedance | $Z_0$ | Ω | 61.485 | 63.02 |
| Surge Impedance loading at 420V | SIL | MVA | 2869 | 2799 |

- **XLPE cable modelling**

To use PSCAD for computing line constant, the XLPE cable must be considered as typical coaxial cable sine PSCAD does not support a structure of XLPE cable under Bergeron model so, first, conversion work is needed to convert XLPE cable to typical coaxial cable for which there are few equations as follows. The geometric dimension of the XLPE cable is selected for 420kV with lead sheath [14].

The conductor is made of annealed copper, and its resistivity ρ is 1.72 × $10^{-8}$ Ωm. To compute line parameters, the resistivity must be increased to compensate the clear space between strands. The solid conductor resistivity can be calculated by the formula [13]

$$\rho_c{}' = \rho \times \frac{\pi \cdot {r_1}^2}{A_c} \quad \text{.....(12)}$$

$\rho_c{}'$ represents increased resistivity, ρ and $A_c$ is the resistivity of material used for the stranded conductor and the cross-section area of the core. Additionally, Semi-conducting layers can be a part of insulation [13] by computing the electrical permittivity.

$$\varepsilon' = \varepsilon_r \times \frac{ln\frac{r_2}{r_1}}{ln\frac{b}{a}} \quad \text{.....(13)}$$

The $r_2$ and $r_1$ is the radius of inner sheath and core respectively. The inner and outer insulated radius are represented by a and b. $\varepsilon_r$ is the permittivity of XLPE as $\varepsilon_r$ = 2.3 [2]. the wired sheath also can be estimated as cylindrical solid conductor [2],[13] with the formula.

$$r_3 = \sqrt{\frac{A_s}{\pi} + {r_2}^2} \quad \ldots\ldots(14)$$

The outer radius $r_3$ can be calculated with the total wire area $A_s$ and inner sheath radius of $r_2$.

Again, the model used for simulation is composed of copper conductor, XLPE insulation, lead sheath, and polyethene outer sheath [14]. Moreover, the parameters are computed at 50 Hz buried in the depth of laying of 1.5m from the ground by Bergeron model. Table 4 shows calculated parameters for XLPE cable by PSCAD.

Table 3 Equivalent Coaxial Cable Model Parameters for XLPE cable

| Modelling for PSCAD | | Units | Values |
|---|---|---|---|
| Core | Cross-section area | $mm^2$ | 1600 |
| | Outer radius | mm | 25.55 |
| | Relative permeability | - | 1 |
| | Resistivity | Ωm | 2.20465$\times 10^{-8}$ |
| Insulation | Outer radius | mm | 55.85 |
| | Relative permeability | - | 1 |
| | Relative permittivity | - | 2.72 |
| Sheath | Outer radius | mm | 60.05 |
| | Resistivity | Ωm | 22$\times 10^{-8}$ |
| | Relative permeability | - | 1 |
| covering | Outer radius | mm | 66.05 |
| | Relative permeability | - | 1 |
| | Relative permittivity | - | 2.3 |

Table 4 Simulated Line Constants for XLPE cable

| Cable parameters | Units | Simulated results |
|---|---|---|
| Resistance | Ω/km | 0.0465 |
| Inductance | mH/km | 0.3778 |
| Capacitance | uF/km | 0.1935 |
| Surge Impedance | Ω | 44.19 |
| SIL at 420kV | MVA | 3992 |

- **OHL modelling**

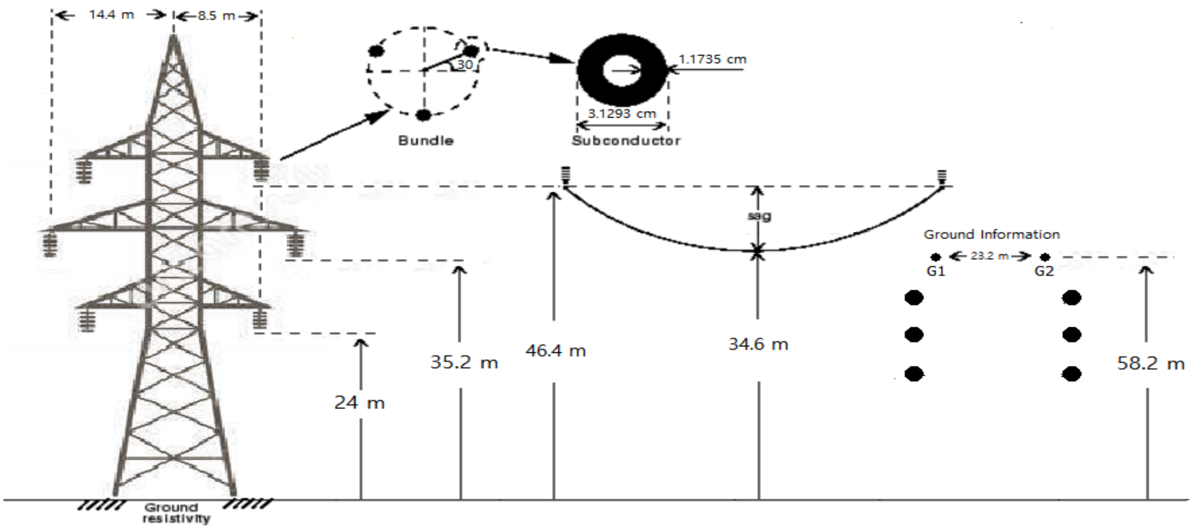


Figure 10 Double-circuit OHL dimensions for simulation using Simulink

Double-circuit overhead line is modelled over RLC line parameters tool in MATLAB with the typical overhead line model for high-voltage up to 500 kV in simulation tool to compute RLC matrixes as well as its sequence parameters for both circuits. The structure of the overhead line is with 6 bundles of 3 ACSR conductors and 2 steel ground wires The DC resistance of a conductor is 0.0521 Ω/km with relative permeability = 1. In the calculation, the conductor's skin effect is included. For the material information of ground wires, its kilometric DC resistance is 4.102 Ω with 1 for relative permeability. The line constant calculation is simulated at 50Hz with 100 Ωm for ground resistivity. The minimum clearance space of ground wire between ground to the wire is 46.4 m, and clearances for the middle conductor and the lowest conductor are 23.4 and 12.2 [m] respectively.

Table 5 Simulated Line Constants for Double-circuit OHL

| Parameters | Units | Simulated value |
|---|---|---|
| Resistance matrix | Ω/km | $\begin{vmatrix} 0.0764 & 0.0667 & 0.0675 \\ 0.0667 & 0.0748 & 0.0667 \\ 0.0675 & 0.0667 & 0.0764 \end{vmatrix}$ |
| Inductance matrix | mH/km | $\begin{vmatrix} 1.1879 & 0.7529 & 0.7352 \\ 0.7529 & 1.1879 & 0.7529 \\ 0.7352 & 0.7529 & 1.1879 \end{vmatrix}$ |
| Capacitance matrix | uF/km | $\begin{vmatrix} 0.0212 & -0.005 & -0.004 \\ -0.005 & 0.0209 & -0.005 \\ -0.004 & -0.005 & 0.0212 \end{vmatrix}$ |

## 3.2. Estimating Maximum Line Length of Transmission Lines

In this section, the maximum capacity of the GIL, XLPE cable and OHL will be estimated by simulation with the parameters calculated in the previous section. To make a quick estimation of the maximum length of transmission technologies [2], each transmission lines are connected by two voltage sources at both ends sending and receiving under the conditions that the thermal current limit is 3190 A as well as 420 $\mathrm{kV_{rms}}$ at both ends. The voltage angle at the receiving end varies according to the line length to hold the thermal current limit of the circuit to be 3190 A, but the angle of sending voltage is fixed at 0.

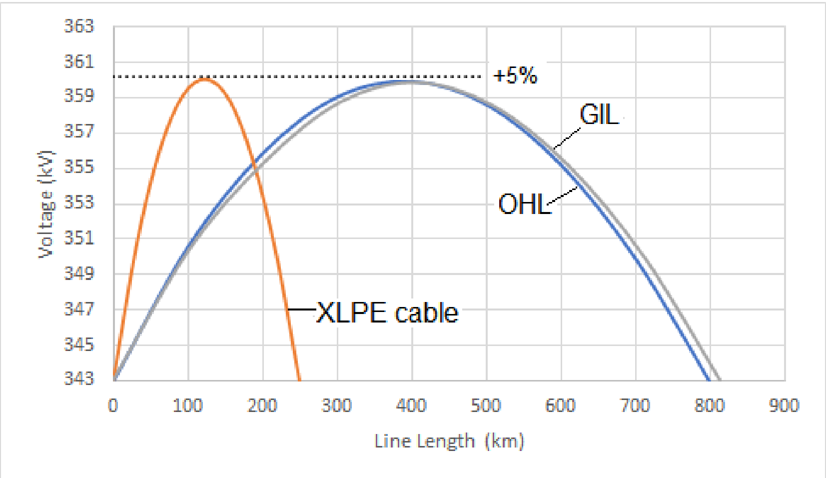


Figure 11 Voltage Profiles for GIL, XLPE cable, and OHL

Figure 9 shows that the voltage increases at the middle of the simulation circuit according to the change of the load angle by the distance when the voltage gain reaches to the voltage limit between +5% to -10% by SQSS [9]. The maximum line length under the voltage limit at the middle of the transmission line to be within +5% to -10% is around 250 km for XLPE cable model and around 800 km for the GIL and OHL.

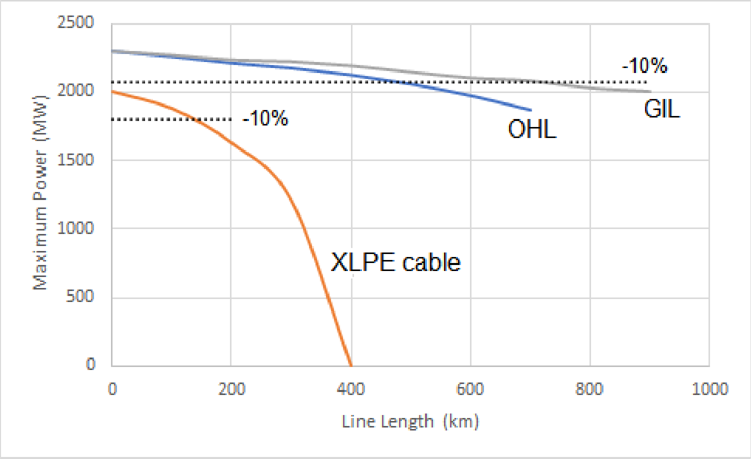


Figure 12 Maximum real power transfer for GIL, XLPE cable, and OHL

As can be seen in figure 11, the line length influences on the maximum real power transmitted that the longer the transmission line is, the bigger the real power drops. The real power can be transferred up to around 750 km for GIL, at which the thermal power rating reaches the minimum limiting line of -10% of its power rating at minimum line length, as well as the maximum line length for OHL, can be estimated as 500 km with simulated model in this project without reactive compensation. For XLPE cable, its power rating reaches the limit when line length of the XLPE cable is around 150 [km]. In this section, the capability of power transfer for the GIL for the long-distance transmission line is verified, and its capability for long distance high power transmission is superior by comparison with existing transmission technologies, XLPE cable, and OHL.

# 4. GIL Simulation

## 4.1. Effect of Different Line Length

### - Simulink simulation model

To figure out the attributes of line length, the GIL model is simulated under 100% load condition at $420\angle 0\ \mathrm{kV_{rms}}$ for sending end voltage, and lagging power factor at 0.8 with GIL line distance from 200 km to 500 km with 100 km as a unit using Simulink

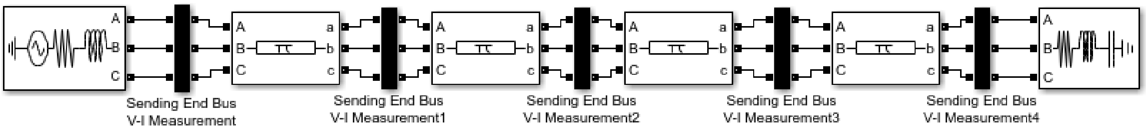


Figure 13 Simulation model for 200 km GIL transmission line using Simulink

Figure 13 represents three-single core GIL lines by a three-phase π section line for 200 km (i.e. each pi-model block represents 50km). The load is connected at the end of the transmission line to operate at 0.8 typical power factor, and the values of the load for each line length are set to attain 0.8 lagging power factor on the thermal current limit 3190 A at 100% loading condition. The amount of the load at the end of the transmission line is given in the table 6 which are used for the simulation. The GIL line developed on Simulink computes voltage, current, real power and reactive power at every 50km. With simulated electrical outputs, the profiles are plotted in Figure 14.

Table 6 Load impedances regarding transmission line length at 0.8 lagging p.f.

| Transmission line length | Load Impedance (Ω) |
|---|---|
| 200km | 39.46+j52.61 |
| 300km | 36.88+j49.17 |
| 400km | 34.52+j46.03 |
| 500km | 32.41+j43.21 |

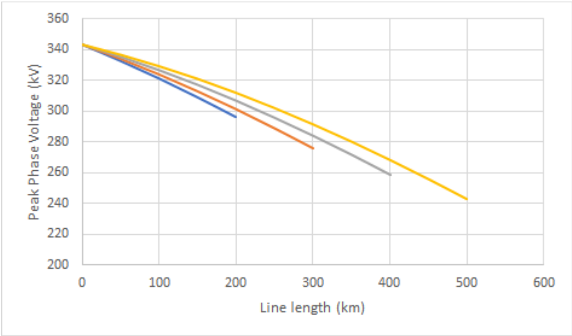


(a) Voltage Drop Profiles

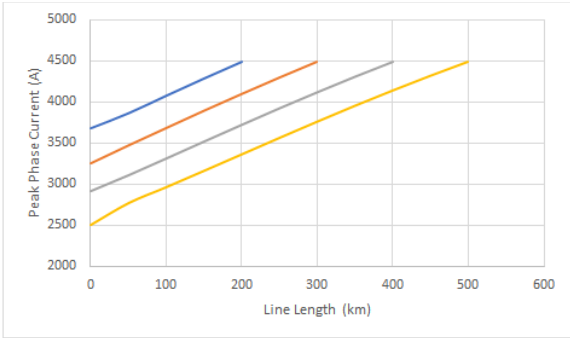


(b) Current Rise Profiles

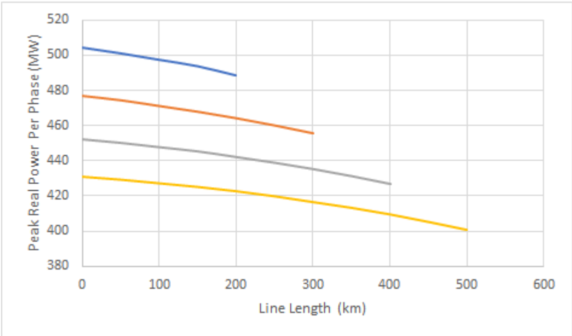


(c) Real Power Losses Profiles

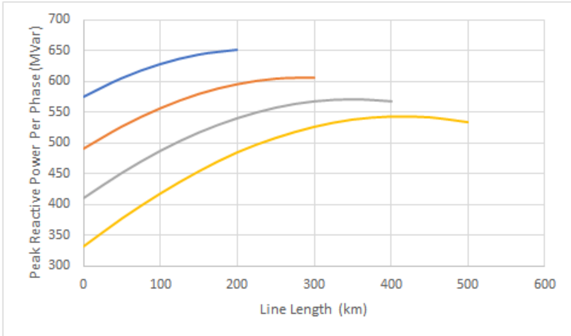


(d) Reactive Power Gain Profiles

Figure 14 Simulink simulation results for electrical power transfer characteristics regarding line length

The change of the electrical power transfer characteristic (i.e. voltage, current, real power, and reactive power in this report) is essential information to analyse the power transmission technology between the sending end and receiving end. The transition of electrical power transfer characteristic is determined by the equation (26) [2].

$$\text{The rate of change } (\%) = \frac{Receiving\ end - Sending\ end}{Sending\ end} \times 100 \ldots\ldots\ldots\ldots\ldots\ldots\ldots\ldots\ldots\ldots\ldots (26)$$

The ratio of voltage drops is computed in table 7 by the equation (26) using each ends magnitude form the voltage profiles in figure 14 – (a). Table 7 shows the range of voltage drops along the transmission line from -13.7 % and -29.2% for line length 200km and 500km respectively and its percentage of voltage drops increases in proportion to line length. All the voltage drops percentages break the bounds of the voltage regulation between +5% and -10% stated SQSS [9]. This is because of additional inductance imposed on the transmission line [2]. To make soft-landing of voltage drop within the range from +5% to -10%, the power factor needs to be improved by shunt capacitive compensation. The power factor lags when an inductive load is linked to the transmission line because of lagging load current. With the method of connecting a shunt capacitor, a leading current that leads the voltage source can be injected [15].

For the current profiles, table 7 shows the percentage of rising current by the current profiles in figure 14 – (b) over different line length with a thermal current limit at receiving end as 3190A under 100% load condition. The rate of rising current increases steeply as from 22.3% at 200km to 74.2% at 500km shown in table 7. The current rise in the transmission line can be explained by charging current imposed on the current by the capacitance of the transmission line [16]. The charging current is significantly small compared to those thermal rating and can be negligible in the relatively short transmission line, but for greater distance high voltage transmission line, the charging current of the transmission line contributes to augment the total thermal current limitation significantly [16]. The relationship between charging current and capacitance for long-distance transmission line can be seen by equation (27) [15].

$I_{chg} = j\omega C_n V_{an}$ $[\mathrm{Ami^{-1}}]$……………………………………………………………………(27)

Where The notation $C_n$ and $V_{an}$ represent the capacitive susceptance, imaginary part of admittance, and the voltage to neutral respectively.

The table 7 shows the GIL has small losses in real power. With 100% load condition, the percentage of real power losses is -3.09% at 200 km and -6.9% at 500 km. Considerable shunt capacitance on a transmission line can be estimated which generates reactive power (i.e. the amount of reactive power generated by shunt capacitance is more significant than the reactive power consumed by the series inductance) [15]. The percentage of reactive power gain at 200km is 13.4% and at 500km is 60.9% as shown in table 7.

In this examination, all the voltage drops in all the lines from 200km to 500km are outside of the voltage regulation by SQSS [9] at 100% load condition with thermal current limit 3190A and 0.8 lagging power factor. To compensate the voltage drop out of the range, the series compensation needs to be employed at the end of the line to reduces the series impedance of the transmission line to reduce the voltage drops by making load-dependent voltage drops limited [15].

Table 7 The change of The Electrical Power Transfer Characteristics (%)

| Line Length (km) | ∆ V (%) | ∆ I (%) | ∆ P (%) | ∆ Q (%) |
|---|---|---|---|---|
| 200 | -13.7 | 22.3 | -3.09 | 13.4 |
| 300 | -19.5 | 38.2 | -4.45 | 23.6 |
| 400 | -24.8 | 53.9 | -5.78 | 38.4 |
| 500 | -29.2 | 74.2 | -6.9 | 60.9 |

- **Investigation of reliability for Simulink GIL simulation model**

In this section, the electrical power transfer characteristics are calculated by MATLAB code, shown in Appendix 9.2 – (iii) to raise the confidence of the simulation by comparison between simulated and calculated results (i.e. simulated results from the previous section and calculated results from MATLAB calculation). The code is based on the hyperbolic form of the long transmission line equations. The series of process is explained as follows [15]. For clarity, the critical method of this section is reproduced from thesis [2, Sect. 4.3.2.].

$$\sinh\theta = \frac{\varepsilon^{\theta}-\epsilon^{-\theta}}{2} \ , \cosh\theta = \frac{\varepsilon^{\theta}+\varepsilon^{-\theta}}{2} \quad \text{.....(15)}$$

$$V = \frac{V_R+I_R Z_C}{2}\varepsilon^{\gamma x} + \frac{V_R-I_R Z_C}{2}\varepsilon^{-\gamma x} \ , I = \frac{V_R/Z_C+I_R}{2}\varepsilon^{\gamma x} + \frac{V_R Z_C-I_R}{2}\varepsilon^{-\gamma x} \quad \text{.....(16)}$$

The convenient form of the equations giving voltage and current along the line shown in the equations (17, 18) can be derived from rearranging both hyperbolic functions in exponential from (15) and equations for RMS values of voltage and current at a specific point along the line at (16).

$$V = V_R cosh\,\gamma x + \ I_R Z_C \sinh\gamma x \quad \text{.....(17)}$$

$$I = I_R cosh\,\gamma x + \frac{V_R}{Z_C}\sinh\gamma x \quad \text{.....(18)}$$

By substituting l into x of the equations (17, 18), the voltage and current at the sending end can be obtained.

$$V_S = V_R cosh\,\gamma l + \ I_R Z_C \sinh\gamma l \quad \text{.....(19)}$$

$$I_S = I_R cosh\,\gamma l + \frac{V_R}{Z_C}\sinh\gamma l \quad \text{.....(20)}$$

By examination of those equations, the generalised circuit constants ABCD can be obtained for the long-distance transmission line.

$$A = \cosh \gamma l \qquad C = \frac{\sinh \gamma l}{Z_C} \qquad B = Z_C \sinh \gamma l \qquad D = \cosh \gamma l \ldots\ldots\ldots\ldots\ldots\ldots\ldots\ldots (21)$$

The total series impedance Z and shunt admittance Y per phase are computed using the electrical parameters simulated in table 2 by MATLAB as well as the values of Characteristic impedance, propagation constant and surge impedance loading are shown in table 8.

Table 8 The electrical line constants for GIL

| Parameters | Notations | Units | Values |
|---|---|---|---|
| Longitudinal impedance | Z=r+jwl | mΩ/km | 7.097+j67.796 |
| Shunt admittance | Y=g+jwc | mS/km | 0+j0.0171 |
| Characteristic Impedance | $Z_0 = \sqrt{Z/Y}$ | Ω | 63.052-j3.29 |
| Propagation Constant | $\gamma = \sqrt{Z \times Y}$ | 1/km | 0.00006+j0.00104 |
| SIL at 420kV | $\mathrm{SIL} = (420e3)^2/\lvert Z_0 \rvert$ | MVA | 2794 |

The $Z_C$ and $\gamma$ in the generalised circuit constants ABCD shown in equation (21) is represented as characteristic impedance and propagation constant respectively. By solving equation both of (19, 20) by substituting circuit constants ABCD (21), the equation for both of end quantities at sending and receiving can be obtained in the equation (22, 23).

$$V_R = A \times V_S - B \times I_S \ldots\ldots\ldots\ldots\ldots\ldots\ldots\ldots\ldots\ldots\ldots\ldots (22)$$

$$I_R = D \times I_S - C \times V_S \ldots\ldots\ldots\ldots\ldots\ldots\ldots\ldots\ldots\ldots\ldots\ldots (23)$$

With the voltage and current of (22, 23), the real power losses and reactive can be calculated by the formula (24, 25)

$$P_R = |V_R||I_R| cos\theta_R \ldots\ldots\ldots\ldots\ldots\ldots\ldots\ldots\ldots\ldots\ldots\ldots (24)$$

$$Q_R = |V_R||I_R| sin\theta_R \ldots\ldots\ldots\ldots\ldots\ldots\ldots\ldots\ldots\ldots\ldots\ldots (25)$$

The $\theta_R$ is represented to show the phase angle by which the voltage leads current. When current is lagging the voltage, the positive values are assigned to the sign of reactive power. the results of this section are on Appendix 9.2 – (i). The both results from simulated and analytical method make an analogous result. Thus, the GIL simulation model using Simulink makes reliable results.

### 4.2. Effect of The Different Load Conditions of GIL for 300 km and 500 km

In this study, the GIL of the length 300 km and 500 km is simulated to evaluate the GIL for long distance transmission line under various load conditions in the range from no loading condition to 120% in every 20%. For each loading condition, the sending end voltage is fixed as $420\angle 0\ \mathrm{kV_{rms}}$ with thermal current limit 3190A at 0.8 lagging power factor. The thermal current limits are calculated regarding loading conditions, and its load impedance is set up to reach lagging p.f. 0.8 at the end of the transmission lines for both distances 300 and 500km as can be seen in table 9. The GIL simulation model using Simulink is used for this simulation, and the results are recorded at every 50km as electrical power transfer characteristics in figure 15 for 300 km and figure 16 for 500 km, as well as its changing magnitude is calculated in table 10 by the equation (26).

Figure 15 and 16 – (a) shows the voltages profiles in which voltage magnitudes at receiving end falls according to the loading condition rising from 0% to 120%. Likewise, the highest voltage is measured at receiving end when the loading condition is 0%, and the lowest voltage is at 120% for both line length conditions. For the 0% and 20% of loading, the phase voltage at receiving end is higher than at sending end for both of loading conditions but only 20% of loading condition for 300km is within the range of +5% and -10% by SQSS [9] as 0.58% as can be seen in table 10-(a). For the case of the rest loading conditions, the voltage drops as line lengths increased, as well as 20% and 40% of loading condition for 300km and 20% for 500km satisfy the voltage drop limit by SQSS [9]. However, it is economically disadvantageous for the provider to operate at low loading condition [17] and gives adverse impacts to the power plant such as decrease of thermal efficiency and produced power in turbine performance [18] for turbine power plant or incomplete combustion and ignition problems for engines.

Regarding current profiles for various loading conditions, the current rises when the loading condition is over 40% for both distance 300km and 500km, but there is no current flowing for loading condition 0% at receiving end. The percentage of rising current in table 10-(b) has the biggest ratio at 40% and 80% loading for 300km and 500km respectively which means the biggest capacitance is on the transmission line at the loading conditions, and it gives rise to the most significant ratio in current rising [2], which can be explained by charging current with its equation (27).

The small power losses are shown in real power profiles in table 10-(c). The drop ratio between sending and receiving end gets gradually bigger by increasing the load, and the most prominent losses are shown at 120% loading condition for both of distances as -5.92% and -10.34% for 300 km and 500 km respectively.

The reactive power gain is the lowest at 100% load condition and has the biggest gain at 40% and 60% load condition for 300km and 500km respectively. The reactive power at receiving end is smaller than at sending end when loading condition is at 120%. This is because of the significant inductive load at receiving end with insufficient line capacitance [15].

Table 9 Thermal Current Limits and Load Impedances regarding Load Conditions for 300 km and 500 km

| Loading Percentage (%) | Thermal Current Limit [A] | $Z_{Load}[\Omega]$ for 300km | $Z_{Load}[\Omega]$ for 500km |
|---|---|---|---|
| 0% | 0 | 0 | 0 |
| 20% | 638 | 228.64+j304.85 | 245+j326.67 |
| 40% | 1276 | 108.79+j145.05 | 112.39+j149.85 |
| 60% | 1914 | 68.96+j91.95 | 68.06+j90.74 |
| 80% | 2552 | 48.86+j65.15 | 4569+j60.93 |
| 100% | 3190 | 36.88+j49.17 | 32.41+j43.21 |
| 120% | 3828 | 28.58+j38.11 | 23.11+j30.81 |

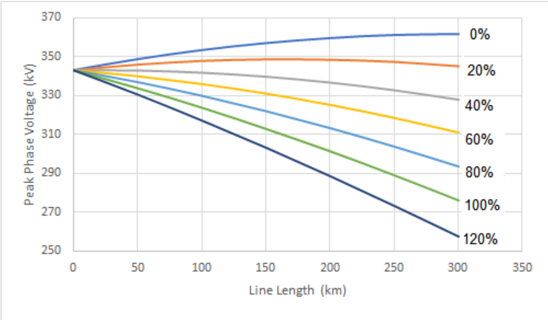


(a) Voltage Profiles for 300km GIL

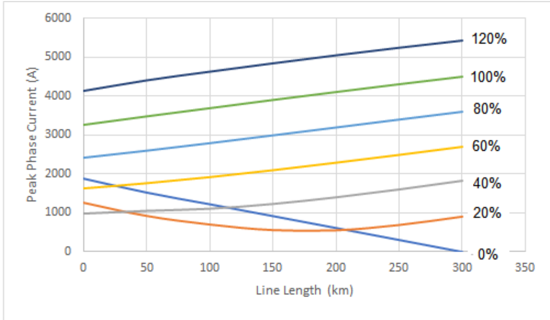


(b) Current Profiles for 300km GIL

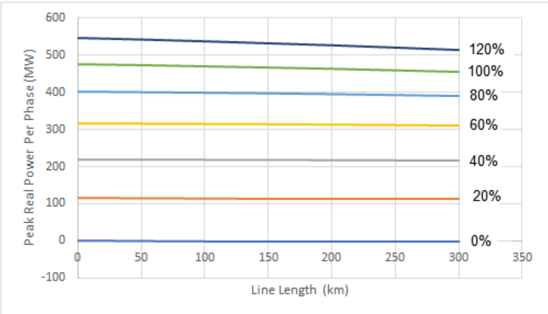


(c) Real Power Profiles for 300km GIL

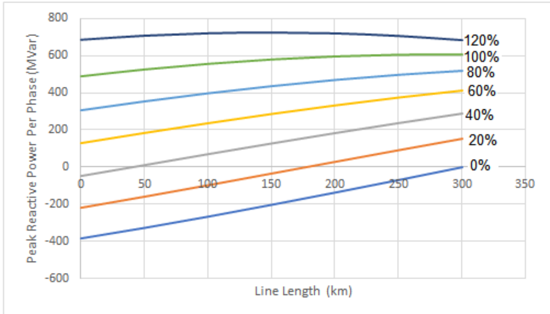


(d) Reactive Power Profiles for 300km GIL

Figure 15 Electrical Power Transfer Characteristics Regarding Different Loading Conditions for 300 km using Simulink

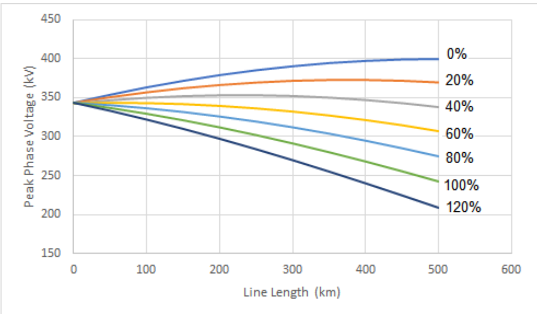


(a) Voltage Profiles for 500km GIL

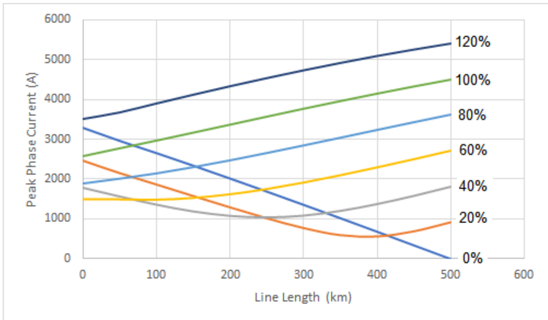


(b) Current Profiles for 500km GIL

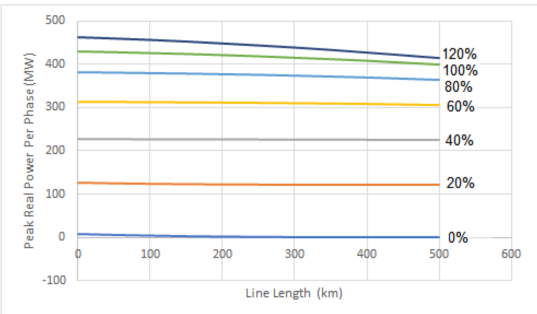


(c) Real Power Profiles for 500km GIL

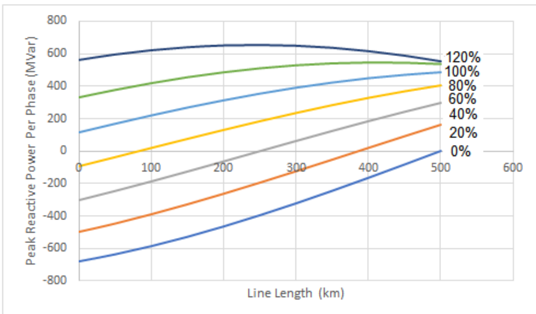


(d) Reactive Power Profiles for 500km GIL

Figure 16 Electrical Power Transfer Characteristics Regarding Different Loading Conditions for 500 km using Simulink

Table 10 The change of The Electrical Power Transfer Characteristics (%)

| (a) Voltage Profiles in different Loading Conditions | | | | | | | |
|---|---|---|---|---|---|---|---|
| Load Condition | 0% | 20% | 40% | 60% | 80% | 100% | 120% |
| ∆ V (%) for 300km | +5.45% | +0.58% | -4.35% | -9.33% | -14.41% | -19.48% | -24.82% |
| ∆ V (%) for 500km | +16.48% | +7.7% | -1.28% | -10.44 | -19.83% | -29.22% | -39.22% |
| **(b) Current Profiles in different Loading Conditions** | | | | | | | |
| Load Condition | 0% | 20% | 40% | 60% | 80% | 100% | 120% |
| ∆ I (%) for 300km | 0% | -28.11% | +84.59% | +67.8% | +49.42% | +38.09% | +31.1% |
| ∆ I (%) for 500km | 0% | -63.3% | +1.29% | +79.58% | +91.61% | +74.21% | +53.68% |
| **(c) Real Power Profiles in different Loading Conditions** | | | | | | | |
| Load Condition | 0% | 20% | 40% | 60% | 80% | 100% | 120% |
| ∆ P (%) for 300km | 0% | -0.67% | -1.09% | -2.02% | -3.14% | -4.45% | -5.92% |
| ∆ P (%) for 500km | 0% | -3.28% | -1.84% | -2.72% | -4.51% | -6.97% | -10.34% |
| **(d) Reactive Power Profiles in different Loading Conditions** | | | | | | | |
| Load Condition | 0% | 20% | 40% | 60% | 80% | 100% | 120% |
| ∆ Q (%) for 300km | 0% | 170.3% | 719.5% | 222.3% | 68.01% | 23.59% | -0.36% |
| ∆ Q (%) for 500km | 0% | 133.1% | 200.2% | 530.4% | 312.5% | 60.77% | -1.53% |

## 4.3. Effect of Different Power Factor of GIL for 300 km and 500 km

In previous simulations, the electrical power flowing of the GIL is studied under different ling lengths or various loading conditions. In this section, the effects of the lagging and leading power factor at unity, 0.98, 0.95, and 0.9 will be studied by GIL simulation model using Simulink. The low power factor is excluded for simulation because the on-site electrical system must be designed to reach the power factor as close as one as possible [20]. The low power factor in a system load results in high internal current and excessive heat and damaging power systems [20]. For both of simulations with lagging and leading power factors, the Simulink with a model in figure 13 is used as the previous simulation at 100% loading conditions with 420∠0kVrms set for sending end voltage for line lengths, 300km and 500km.

### 4.3.1. Lagging power factor

The loads are connected at the end of the GIL simulation model with the impedances in Table 11 at different lagging power factors, unity, 0.98, 0.95 and 0.9. The electrical power transfer characteristics of the simulation are plotted in Figure 17 and 18. The voltage profile shown in the figure 17 and 18 - (a) and table 12-(a) indicates that the receiving end voltage increases according to the power factor as close as near unity, and there is voltage gain when the line length is 500km at unity power factor unlike 300km line length at unity power factor.

When it comes to the percentage of voltage drop, the size of voltage drops grows as lagging power factor decreased for both distances. For 300km, the voltage variation is within +5% to -10% at the unity factor, 0.98, and 0.95 by -1.2, -6.74, and -7.49% respectively. The GIL model built using Simulink for 300km can be operated when lagging power factor is bigger than 0.95 without any reactive compensation. For 500km, the change of voltage is +2.45% at unity power factor and -9.07% at 0.98 power factor, this variation is acceptable by SQSS [9]. So, the GIL model can be run for 500km at the lagging power factor above 0.98 without reactive compensation on the transmission line.

In the table 12-(b), the current increases at the lagging power factors 0.98, 0.95, and 0.9 which means the capacitive line generates current that is imposed on the current of the transmission line for both line distance. However, it can be seen from table 12 – (b) that there is a current drop at unity power factor. This is because of current flowing over the line with pure resistance [15].

The table 12-(c) shows the real power profiles. The biggest loss of real power is at 0.9 lagging power factor by -3.14% and -5.03% for both line length 300km and 500km respectively. The losses ratio increases at the lower power factors from the unity, but the power losses over power factor is relatively small over the simulated lagging power factors for both distances.

As can be seen in figure 17 and 18 - (d), the reactive power converges on 0 at the receiving end for both line lengths at unity power factor. At 0.98 power factor, both lines have the biggest ratio in the reactive power gain, and it decreases as power factor decreases. The reactive power increases in all power factor apart from the unity which means the line is capacitive, and the capacitive line along the transmission line acts as reactive generator [15]. The lagging load requires reactive power which is called demand reactive power and the reactive power at the receiving end can be computed by supplied reactive power subtracted by demand reactive power as can be seen by equation (28) [20]. The reactive power increases along the transmission line because of demand reactive power and the demand reactive power also influences to the receiving voltage by equation (29) [20].

$$Q_R = Q_D - Q_S \quad \text{.....(28)}$$

$$V_R = \frac{V_S}{2} + \sqrt{\frac{{V_S}^2 - 4X_L Q_R}{2}} \quad \text{.....(29)}$$

Where the $Q_R$ is received reactive power, $Q_D$ and $Q_S$ indicates demand reactive power and supplied reactive power respectively.

Table 11 Load Impedances regarding Different Lagging p.f. for 300 km and 500 km

| Lagging Power factor | $Z_{Load}[\Omega]$ for 300km | $Z_{Load}[\Omega]$ for 500km |
|---|---|---|
| Unity | 77+j0 | 87.5 |
| 0.98 | 69+j14.13 | 68+j13.42 |
| 0.95 | 67+j17.28 | 62.5+j20.41 |
| 0.9 | 60+j29.52 | 56.5+j26.69 |

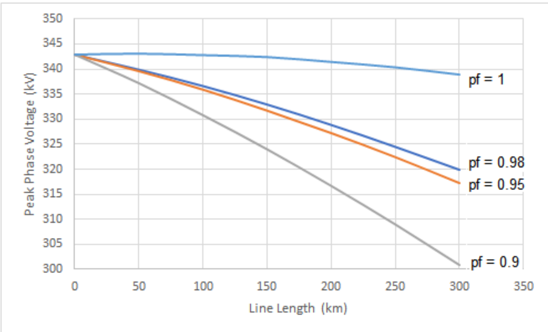


(a) Voltage Profiles for 300km GIL

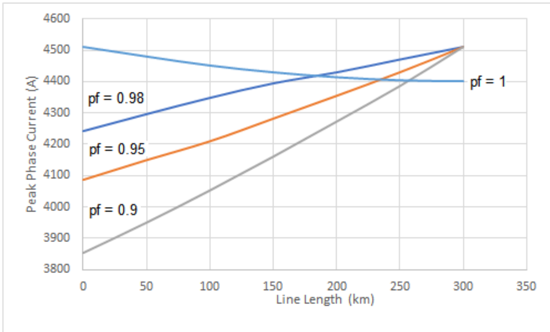


(b) Current Profiles for 300km GIL

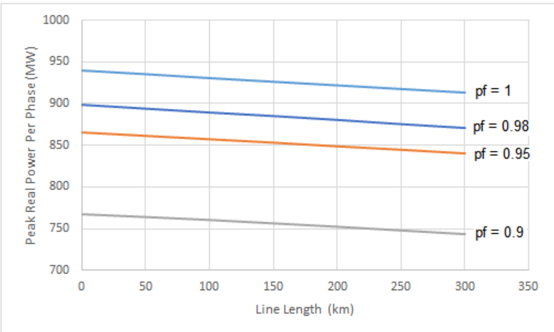


(c) Real Power Profiles for 300km GIL

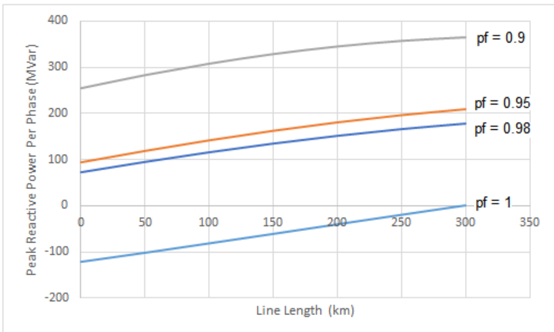


(d) Reactive Power Profiles for 300km GIL

Figure 17 Electrical Power Transfer Characteristics Regarding Different Lagging p.f. for 300 km using Simulink

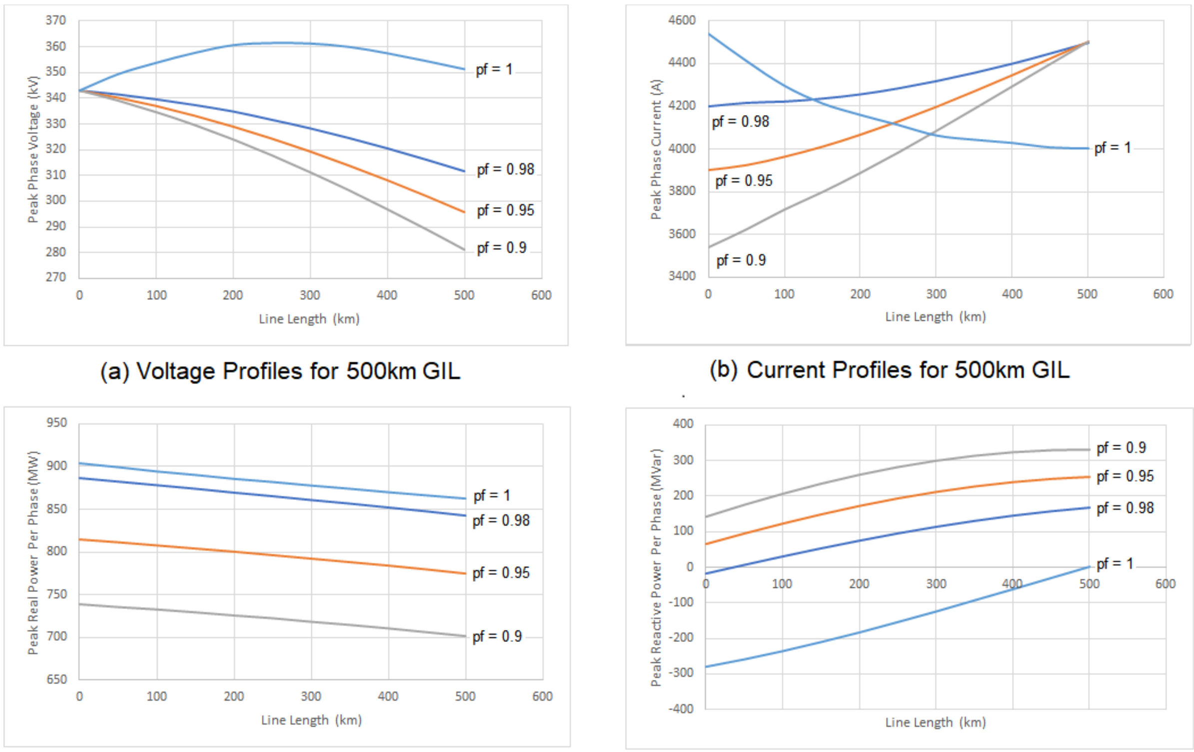


(a) Voltage Profiles for 500km GIL

(b) Current Profiles for 500km GIL

(c) Real Power Profiles for 500km GIL

(d) Reactive Power Profiles for 500km GIL

Figure 18 Electrical Power Transfer Characteristics Regarding Different Lagging p.f. for 500 km using Simulink

Table 12 The change of The Electrical Power Transfer Characteristics (%)

| | | | | |
|---|---|---|---|---|
| **(a) Voltage Profiles in Different Lagging Power factor** | | | | |
| Power factor | Unity | 0.98 | 0.95 | 0.9 |
| ∆ V (%) for 300km | -1.2% | -6.74 | -7.49 | -12.25 |
| ∆ V (%) for 500km | 2.45 | -9.07 | -13.71 | -17.96 |
| **(b) Current Profiles in Different Lagging Power factor** | | | | |
| Power factor | Unity | 0.98 | 0.95 | 0.9 |
| ∆ I (%) for 300km | -2.46% | 6.32% | 10.37% | 17.11% |
| ∆ I (%) for 500km | -11.83% | 7.12% | 15.35% | 27.25% |
| **(c) Real Power Profiles in Different Lagging Power factor** | | | | |
| Power factor | Unity | 0.98 | 0.95 | 0.9 |
| ∆ P (%) for 300km | -2.91% | -3% | -2.92% | -3.14% |
| ∆ P (%) for 500km | -4.52% | -4.88% | -4.91% | -5.03% |
| **(d) Reactive Power Profiles in Different Lagging Power factor** | | | | |
| Power factor | Unity | 0.98 | 0.95 | 0.9 |
| ∆ Q (%) for 300km | 0% | 144.7% | 121% | 43.97% |
| ∆ Q (%) for 500km | 0% | 1009% | 280.6% | 133.3% |

### 4.3.2. Leading power factor

To investigate the effects of leading power factor, the sending end voltage of a GIL simulation model is $420\angle 0\ \mathrm{kV_{rms}}$ at various leading factors for line length 300km and 500km at 100% loading condition. The loads at the end of the transmission line are set up by resistance and capacitance which are shown in table 13. The electrical power transfer characteristics (i.e. voltage, current, real power, and reactive power) are plotted in figure 19 for 300 km and 20 for 500 km, and its ratio of variations between sending and receiving end is calculated in table 14.

Differently, to the lagging power factor, voltage increases along the transmission line in leading power factor apart from the voltage for 300km at 1 and 0.98 leading p.f. as shown in the table 14-(a). For 300km, the change of voltage is within the voltage drop limit between +5% to -10% at all the leading power factor simulated. In contrast, for 500km, voltage gain at only unity power factor is in the range by 2.45% of the SQSS for Planning and operating offshore transmission system [9]. In regards the current profiles, the current increases at receiving end and the change of current variation increases as power factor fallen. The current usually is ahead of the voltage regarding phase because power system is generally operated by lagging power factor. But in the leading power factor, the voltage leads the current since there are significant line capacitance and capacitor capacity [15]. In this case, the voltage at receiving end is bigger than sending voltage. This phenomenon is called ‘Ferranti effect’ [22]. There are a few drawbacks from the effect such as increasing of power losses, transformer power loss, and system voltage.

For the real power and reactive power profiles, the real power losses are still small as previous simulations despite the Ferranti effect. For the reactive power, it has a convergence on the 0 for all the power factor in this simulation.

Table 13 Load Impedances regarding Different Leading p.f. for 300 km and 500 km

| Leading Power factor | $Z_{Load}[\Omega]$ for 300km | $Z_{Load}[\Omega]$ for 500km |
|---|---|---|
| Unity | 77-j0 | 87.5-j0 |
| 0.98 | 88.25-j0.0568 | 127-j0.0393 |
| 0.95 | 93.5-j0.0327 | 152.8-j0.0201 |
| 0.9 | 97.5-j0.0214 | 176-j0.0122 |

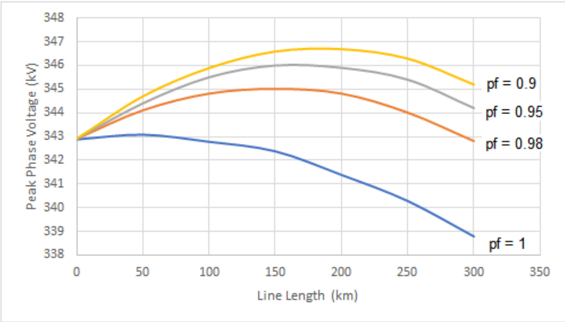


(a) Voltage Profiles for 300km GIL

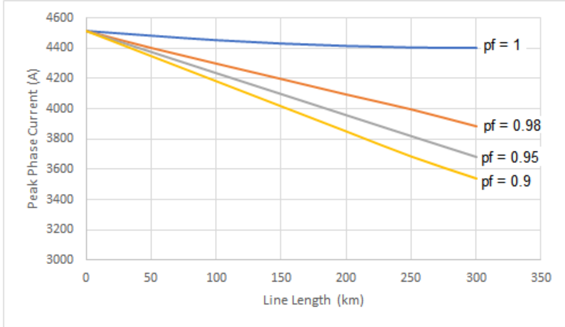


(b) Current Profiles for 300km GIL

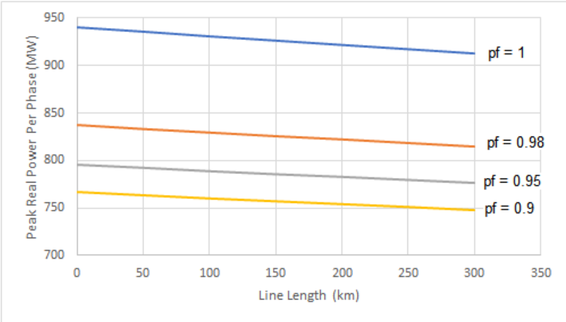


(c) Real Power Profiles for 300km GIL

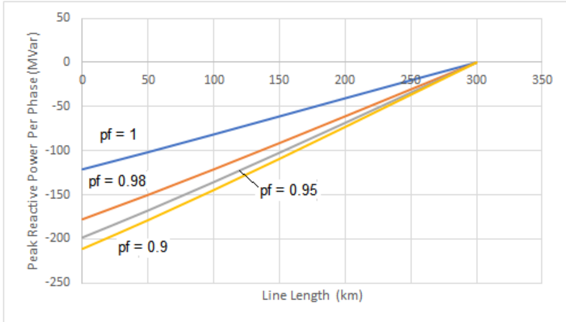


(d) Reactive Power Profiles for 300km GIL

Figure 19 Electrical Power Transfer Characteristics Regarding Different Leading p.f. for 300 km using Simulink

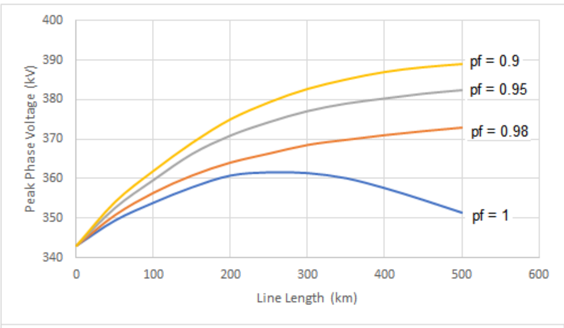


(a) Voltage Profiles for 500km GIL

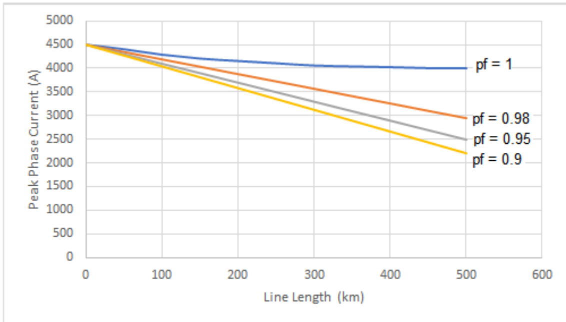


(b) Current Profiles for 500km GIL

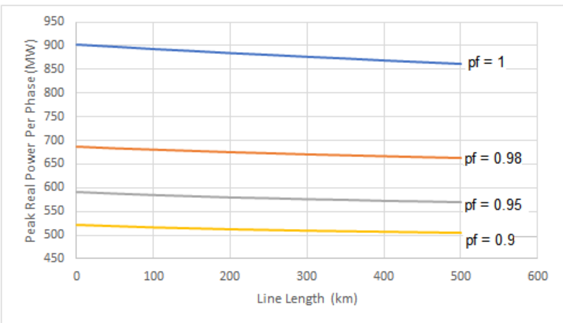


(c) Real Power Profiles for 500km GIL

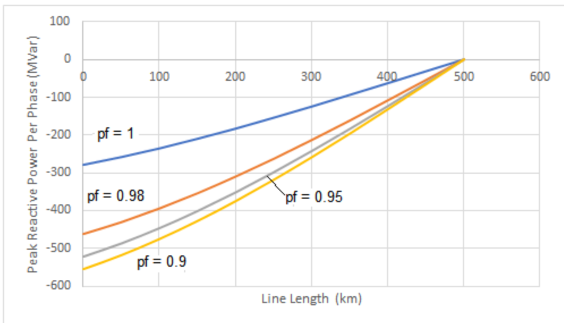


(d) Reactive Power Profiles for 500km GIL

Figure 20 Electrical Power Transfer Characteristics Regarding Different Leading p.f. for 500 km using Simulink

Table 14 The change of The Electrical Power Transfer Characteristics (%)

| (a) Voltage Profiles in Different Leading Power factor | | | | |
|---|---|---|---|---|
| Power factor | Unity | 0.98 | 0.95 | 0.9 |
| ∆ V (%) for 300km | -1.2% | -0.03% | 0.38% | 0.67% |
| ∆ V (%) for 500km | 2.45% | 8.78% | 11.52% | 13.44% |
| **(b) Current Profiles in Different Leading Power factor** | | | | |
| Power factor | Unity | 0.98 | 0.95 | 0.9 |
| ∆ I (%) for 300km | -2.46% | -13.88% | -18.38% | -21.5% |
| ∆ I (%) for 500km | -11.24% | -34.89% | -44.41% | -51.01% |
| **(c) Real Power Profiles in Different Leading Power factor** | | | | |
| Power factor | Unity | 0.98 | 0.95 | 0.9 |
| ∆ P (%) for 300km | -2.91% | -2.63% | -2.46% | -2.4% |
| ∆ P (%) for 500km | -4.52% | -3.68% | -3.53% | -3.44% |
| **(d) Reactive Power Profiles in Different Leading Power factor** | | | | |
| Power factor | Unity | 0.98 | 0.95 | 0.9 |
| ∆ Q (%) for 300km | 0% | 99.7% | 99.86% | 99.92% |
| ∆ Q (%) for 500km | 0% | 99.96% | 99.99% | 99.99% |

## 4.4. Summary

The electrical power transfer characteristics of the GIL are evaluated in this section regarding different line lengths, loading conditions and lagging/leading power factor. The simulations show that the GIL can be operated without reactive compensation under specific conditions within the range of voltage drop limits from +5% to -10% by SQSS for planning and operating offshore transmission systems [9]. The available GIL circumstances are indicated by shaded cells in table 15.

Although it is economically disadvantageous to operate at low loading conditions, The GIL can be operated at 20%, 40% and 60% loads for 300km and 40% for 500km without reactive compensation as can be seen in the table 15-(a). In regards lagging power factor when the power factor is close to unity for both line length, the voltage drop of the GIL is within the drop limit. In leading power factor, the GIL can be operated at all power factors from 1 to 0.9 for 300km, and at power factor 1 and 0.98 for 500km but operation in leading factor has many disadvantages because of Ferranti effect.

Table 15 Rearrangement of the change of voltage between sending end and receiving end at different conditions (shaded blocks show the voltage variation is within the range between +5% and -10% stated by SQSS [9]).

(a) Effects of Different Line Lengths

| Inherent Variability – Lagging Power factor 0.8, Loading condition 100% | | | | |
|---|---|---|---|---|
| Line length (km) | 200 | 300 | 400 | 500 |
| ∆ V (%) | -13.7 | -19.5 | -24.8 | -29.2 |

(b) Effects of Different Loading Conditions

| Inherent Variability – Lagging Power factor 0.8, Line length 300km,500km | | | | | | | |
|---|---|---|---|---|---|---|---|
| Loading | 0% | 20% | 40% | 60% | 80% | 100% | 120% |
| ∆ V (%) for 300km | -5.45 | +0.58 | -4.35 | -9.33 | -14.41 | -19.48 | -24.82 |
| ∆ V (%) for 500km | +16.5 | +7.7 | -1.28 | -10.44 | -19.83 | -29.22 | -39.22 |

(c) Effects of Different Lagging Power Factors

| Inherent Variability –Line length 300km,500km, Loading condition 100% | | | | |
|---|---|---|---|---|
| Lagging power factor | Unity | 0.98 | 0.95 | 0.9 |
| ∆ V (%) for 300km | -1.2 | -6.74 | -7.49 | -12.25 |
| ∆ V (%) for 500km | 2.45 | -9.07 | -13.71 | -17.96 |

(d) Effects of Different Leading Power Factors

| Inherent Variability –Line length 300km,500km, Loading condition 100% | | | | |
|---|---|---|---|---|
| Leading power factor | Unity | 0.98 | 0.95 | 0.9 |
| ∆ V (%) for 300km | -1.2 | -0.03 | 0.38 | 0.67 |
| ∆ V (%) for 500km | 2.45 | 8.78 | 11.52 | 13.44 |

# 5. Costs Comparison in Transmission Systems

Until now, electrical characteristics of The GIL has been studied but the electrical capability of the GIL is a not only vital aspect to be used to evaluate GIL as an alternative technology, but its economic issues must be considered as well. To study the costs of the GIL, XLPE cable and OHL for transmission lines for offshore wind power, some useful information and data from the various renewable energy industry in the UK is employed. The average capacity factor is used for the UK offshore wind - farms as 33.6% [23] measured from the date of Oct 2016 to Oct 2017. Moreover, the offshore operational capacity is 6,713.52 MW from 1,832 offshore turbines in the UK on 18 April 2018, offered by UK Energy Database (UKWED) [22]. The cost per MWh varies within the range between around ￡30 to ￡65 per MWh [24] from which mean value is chosen in this section as ￡48.0 per MWh [24]. The lifetime of GIL, XLPE cable and OHL are assumed to be over the nominal 40 years with the system AC voltage 400kV for 75km. In the calculation, the laying method for GIL is tunnel-laid and direct-buried, as well as the XLPE cable is considered as direct-buried AC underground cable. Additionally, the cost of operation and maintenance is assumed to be ￡0 since the oldest direct-buried GIL has been running without any substantial maintenance required for over 40 years [1]. Table 16 shows the installation costs per kilometre and the operation and maintenance costs per year for each transmission technologies. To calculate lifetime costs for transmission lines, the equation (30) [25] is used with the electrical parameters simulated in section 3. The value of losses caused by fuel efficiency is excluded as wind power used.

$$C_{tot} = \mathrm{CDC} + \mathrm{CL} + \mathrm{COM} \quad \text{(30)}$$

where $C_{tot}$ is total lifetime cost, CDC is the total capital cost of the installation, CL is Net Present Value(NPV) of the cost of losses and COM is Net Present Value(NPV) of the typical cost of operation and maintenance

Table 16 Major Costs Information for Transmission technologies [27]

| Costs | GIL-tunnel laid | GIL–direct buried | XLPE cable | OHL |
|---|---|---|---|---|
| Installation Costs (￡/km) | ￡22.93m | ￡16.2m | ￡18.14m | ￡1.795m |
| Operation and Maintenance Costs (￡/year) | ￡0.745m | ￡0m | ￡0.435m | ￡0.123m |

## 5.1. Lifetime cost calculations for the GIL, XLPE cable, OHL

For the tunnel-laid GIL costs calculation for 40-years as a beginning, the total costs over a lifetime will be calculated by the equation (30), suggested by Western Power Distribution [25], for which the calculation procedure will be presented for CDC, CL, and COM as follows

- **Computing CDC**

The equation (31) can calculate the capital cost of equipment(CDC).

CDC = Construction Line Length (75km) × cost per km ( £ 22.93m)……………….(31)

So, the value of CDC can be obtained as £ 1719.75m

- **Computing CL**

For calculating CL, cost of losses, there are six steps as follows

1st step – computing the average loading

Average loading (MW) = Circuit Capacity (MW) × Average utilisation......…………..(32)

$$\text{Average Loading (MW)} = \frac{6{,}713.52 \times 33.6}{100} = 2255.74 \text{ MW}$$

2nd step – computing the average current

Average current (A) = Average loading (kW)/Operating Voltage (kV) × $\sqrt{3}$....……...(33)

Average current (A) $= \frac{2255.74 \times 1000}{400 \times \sqrt{3}} = 3255.9 \text{ Amps}$

3rd step – computing the resistance of the circuit

The resistance to circuit = resistance ($\Omega m^{-1}$) × Line Length(km).....…………………(34)

So, the resistance of the GIL can be calculated as 0.567 Ω for 75 km.

4th step – computing the three-phase lost power

Line losses(kW) = 3× $Average\ Current^2 \times Line\ resistance$/1000…...………………..(35)

Line losses(kW)$= \frac{3 \times 3255.9^2 \times 0.567}{1000} = 18032.11\text{kW}$

5th step – computing annual cost of losses

The annual cost of losses = Lost power(MW) ×24hr×365days×Cost per MWh…..(36)

The annual cost of losses = $\frac{18032.11\times24\times365\times48}{1000} = £7.582\text{m}$

6th step - computing net present value of the cost of losses

Net Present Value is computed with a discount rate 3.5% [26] over 40 years

By the steps, the value of CL can be calculated as £164.5m

- **Computing COM**

Cost of operation and maintenance (COM)

Operation and maintenance costs= Period (years) ×Average Costs per year……..(37)

Operation and maintenance costs per year $= 40 \times 0.745\text{m} = £29.8\text{m}$

The Net Present Value of cost of operation and maintenance for 40 years lifetime can be computed using a discount rate of 3.5% [26]

So, COM is calculated as $£64.667\text{m}$

- **Computing $\boldsymbol{C_{tot}}$**

So, by taking account of those calculations, the total cost over a lifetime for a 75 km transmission line of the tunnel-laid GIL can be estimated by the total lifetime cost ($C_{tot}$ ) and the total Lifetime cost is $£1948.72\text{m}$. By the same procedure, the lifetime costs for direct-buried GIL, XLPE cable, and OHL can be calculated in table 17. The calculated lifetime cost for each transmission technologies is shown in table 17. Again, the notations in table 17, $C_{tot}$, CDC, CL and, COM are expressed in the equation (30). The table 18 shows the ratio between OHL and other transmission technologies.

Table 17 Calculated Costs of $C_{tot}$, CDC, CL, and COM

| Costs | $C_{tot}$ | CDC | CL | COM |
|---|---|---|---|---|
| GIL – tunnel laid | £1948.7m | £1719.8m | £164.5m | £646.7m |
| GIL – direct buried | £1379.5m | £1215m | £164.5m | £0m |
| XLPE cable | £2750.1m | £1360.5m | £1012m | £377.6m |
| OHL | £435.3m | £134.6m | £193.9m | £106.8m |

Table 18 Transmission Technology Cost Ratios

| Transmission Technology | Lifetime Cost Factor (x: OHL) |
|---|---|
| Tunnel Laid GIL | 4.48 |
| Direct Buried GIL | 3.17 |
| XLPE cable | 6.32 |
| OHL | 1 |

## 5.2. Cost comparison

When it comes to the total capital cost for installation (CDC), The tunnel-laid GIL is the most expensive between those technologies by £1719.8m shown in table 17. This is mainly because the extra cost for tunnelling construction is imposed on the build costs which makes the installation costs of GIL technology much more sensitive by route length. The installation costs for the overhead line is significantly cheaper than other three transmission technologies laying under the ground by £134.6m since on route installation cost is considerably less expensive and the direct-buried GIL is the second cheapest by £1379.5m.

In regards the net present value of the cost of losses (CL) the XLPE cable technology is much expensive than other two technologies by £1012m because the resistance of the XLPE is much more significant than GIL and OHL and this results in considerable power losses. Unlike the XLPE cable technology, the cost of losses in the GIL and OHL are relatively inexpensive by ￡164.5m (i.e. cost of losses is identical for tunnel-laid and direct-buried GIL) and ￡193.9m respectively.

For Net Present Value(NPV) of the cost of operation and maintenance (COM), the tunnel-laid GIL has the most expensive operation and maintenance cost over a lifetime by ￡193.9m (however, the operation and maintenance cost for direct-buried is assumed as ￡0 in this report). Sequentially, XLPE cable and OHL are expensive by ￡377.6m and ￡106.8m respectively.

Overall, although the costs of installation (CDC) and operation and maintenance (COM) for the tunnel-laid GIL is the most expensive when compared to XLPE cable, OHL, the total lifetime cost of the GIL is cheaper than XLPE cable. This is because the total lifetime cost, 40 years, of XLPE cable, is considerably increased by the net present value of the cost of losses (CL) by its significant power losses by high resistance. Additionally, the total life cost of direct-buried GIL is cheaper than both of transmission technologies because this technology can save costs from tunnelling and operation and maintenance. The total lifetime cost for OHL is the most cheaper than The GIL and XLPE cable by ￡435.3m as can be seen in table 17. In cost aspect, the OHL is cheaper than both of transmission technologies by 3.17 times than direct-buried GIL and by 6.32 times than XLPE underground cable.

# 6. Discussion

In this report, the investigation was carried out for a comprehensive evaluation of GIL by studying maximum real power transfer and lifetime costs for GIL, XLPE cable, and OHL under the advantages for social environment of the GIL already established, mentioned in the literature review in section 2.1.

The GIL modelling is carried out in section 3.1, as well as its line parameters are simulated using PSCAD. Comparison with calculated parameter values proved the reasonable reliability of simulated results. The GIL has the lowest resistance to transmission technologies. This is because of the wider cross-section area of the GIL.

With the lowest resistance of the GIL, it is demonstrated in section 3.2 that the GIL has a high capability for long distance transmission line up to around 750 km simulated using Simulink. On the other hand, the power transmit capability for XLPE cable and OHL is up to around 150 km and 500 km respectively. This result shows both technologies XLPE cable and OHL fall behind in maximum transmission capability. Especially, transmission capability of the GIL is significantly outstanding in comparison to XLPE cable.

The electrical transmission characteristic of the GIL has been evaluated in section 4 regarding three cases of the GIL in different line length, load condition, and power factor by simulation using Simulink and MATLAB. The MATLAB was used to make a mathematical result with which the reliability of GIL simulation model was demonstrated that those have similar results apart from the magnitude of real power and reactive power. As a result, in section 4, the GIL can be operated for the offshore wind farm transmission line (300km) without reactive compensation on the conditions that:

- Low loading conditions from 20% to 60% at lagging power factor 0.8
- From 0.95 lagging p.f. to 0.9 leading p.f. at 100% loading condition

The total lifetime costs of tunnel-laid and direct-buried GIL, XLPE cable, and OHL is ￡1948.7m, ￡1379.5m, ￡2750.1m, and ￡435.3m respectively. The total lifetime costs show that the GIL is not the most expensive if the technologies are used for a long period since the GIL has the lowest power losses between those. The OHL is the cheapest, but the OHL has its inherent uncertainty during lifetime since the OHL is exposed to the outside and this results in making OHL sensitivity to environmental and climate. Additionally, the cost for GIL can be reduced by using higher voltage. The installation cost for direct-buried GIL in this report is nine times expensive than OHL. However, this cost factor can be decreased to 2 to 3 times if the higher voltage level of 1000 kV is used [1]. Thus, the GIL technology shows high-cost competitiveness with its high reliability and small power losses. Thus, the GIL technology is much more economical when the higher voltage is rated or constructed for the longer-term aim.

## 7. Conclusion

This project is to study the suitability of the GIL for an alternative of the OHL from the drawbacks mentioned in the motivation. The capability of power transmission of the GIL is remarkable even more than OHL although total lifetime costs of GIL is expensive (i.e. the primary advantage of GIL is bulk power transmission for long distance). However, the GIL will be a sound investment if equipment investor takes consideration of its high reliability and long-term operational lifetime (Additionally, the GIL’s economic drawback can be tackled by using higher voltage). Undoubtedly, the gas insulated transmission line is suitable for an alternative technology for long distance bulk-power transfer. Moreover, this technology has a potential to overwhelm other transmission systems in term long term if further research can be carried on its SF6 insulation gas to be much closer to eco-environmental technology.

# 8. References


[1] Koch, H “Gas insulated transmission lines (GIL)”, IEEE Xplore, distributor, & John Wiley & Sons, publisher, 2015.

[2] Elnaddab, K. “Evaluation of Gas Insulated Lines (GIL) for Long Distance HVAC Power Transfer “, PhD. Thesis, Cardiff University, UK, 2015

[3] Koch, H. “Experience with 2nd Generation Gas-Insulated Transmission Lines GIL [PDF]. Erlangen Germany: Siemens AG, n.d.

[4] “Gas-insulated transmission lines”, Siemens technical brochure, Erlangen (Germany), n.d.

[5] “Compressed Gas Insulated Transmission Bus Systems”, CGIT technical brochure, Massachusetts (USA), 2002

[6] Rahman. A.H et al. “Comparison of Voltage Regulation of Gas Insulated Transmission Line and XLPE Cable”, International Journal of Modern Trends in Engineering and Research (IJMTER) Volume 02, Issue 04, 2015.

[7] Benato, R., Paolucci, Antonio. “EHV AC Undergrounding Electrical Power Performance and Planning (Power Systems)”, Springer, 2010.

[8] Benato, R., Dughiero, F., Forzan, M., & Paolucci, A. “Proximity effect and magnetic field calculation in GIL and in isolated phase bus ducts”, Magnetics, IEEE Transactions on,38(2), 781-784, 2002.

[9] National Grid, “National Electricity Transmission System Security and Quality of Supply Standard,” 2012.

[10] Patel, V., & Jamnani, J. “Techniques to increase Surge Impedance Loading level of EHV AC transmission lines for improving power transfer capability”. Computation of Power, Energy Information and Communication (ICCPEIC), 2015 International Conference on, 0518-0523, 2015.

[11] Gudmundsdottir, U. S. “Modelling of ling High Voltage AC Cables in the Transmission System”, Department of Energy Technology, Aalborg University, 2010.

[12] "Bergeron Model", Hvdc.ca. [Online] Available: https://hvdc.ca/webhelp/Master_Library_Models/Transmission_Lines_Cables/Distributed_Line_Models/bergeron_options.htm.

[13] Silva and L. Kothalawala, "Modelling Cables and Transmission Lines with PSCAD™/EMTDC™", WEBINAR.

[14] “LS EHV Cable System 66~500kV Cable and Accessories”, LS cable sales brochure, Anyang (S. Korea), 2009.

[15] Grainger, J., & Stevenson, William D. “Power system analysis”. New York ; London: McGraw-Hill, 1994

[16] Schifreen, C., & Marble, W. Charging-current limitations in cable lines. Electrical Engineering, 75(6), 511, 1956.

[17] Tufte. E. D. “Impacts of Low Load Operation of Modern Four-Stroke Diesel Engines in Generator Configuration “, MSc dissertation, Norwegian University of Science and Technology, Norway, 2014.

[18] Karakurt, A. S., & Güneş, Performance analysis of a steam turbine power plant at part load conditions. Journal of Thermal Engineering, 3(2), 1121-1128. 2017.

[19] “The Effect of Power Factor on An Electrical System”, MTU onsite energy technical brochure, Germany, n.d.

[20] Maitra. S. “Reactive Power and Voltage Relationship in Power Transmission Line” [Video File]. Retrieved from: https://www.youtube.com/watch?v=LwUjt5-8D4mw, 2017.

[21] “The Problem of Leading Power Factor”, Samwha capacitor co. technical brochure, n.d.

[22] R. Association, "Wind Energy Statistics - RenewableUK", Renewableuk.com. [Online]. Available: http://www.renewableuk.com/page/UKWEDhome.

[23] "UK offshore wind capacity factors – a semi-statistical analysis", Energy Matters. [Online]. Available: http://euanmearns.com/uk-offshore-wind-capacity-factors-a-semi-statistical-analysis/. [Accessed: 21- Apr- 2018].

[24] UK Energy Research Centre, "A REVIEW OF ELECTRICITY UNIT COST ESTIMATES", UK, 2007.

[25] “Lifetime Costs Report – Brechfa Forest Connection Project”, Western Power Distribution project report, UK, 2014.

[26] “Management of Electricity Distribution Network Losses”, Imperial College London, Sohn associates, UK, 2014.

[27] Brinckerhoff. P. “Electricity Transmission Costing Study – report and appendices”, UK, 2012.

# 9. Appendices

## 9.1. Appendix 1 – Progress Report

The University of Manchester

Evaluation of GIL for long distance bulk-power transmission

Third Year Individual Project – Progress Report

Nov 2017

**Seunghwan Kim**

9767991

Supervisor: Dr. Tony lujia Chen

School of Electrical and Electronic Engineering

**Contents**

# 1. Introduction

## 1.1. Motivation.

In 1974, the gas-insulated transmission line was designed from Gas insulted switchgear to connect between electric transformer and overhead electric line at hydroelectric power plant in Schluchsee, Germany. It has been used for the last 40 years [1]. But, this technology could not get a lot of attention except for cases for a long time. This is because of lack of demand of GIL as well as relatively easiness of construction in overhead line which causes catalyst reduction of interest of it. However, nowadays, the GIL has a high company's visibility since the power companies face difficulties in securing new land to construct overhead lines as well as increasing the environmental civil complaint by expansion of metropolis and by consciousness of environment from overhead transmission line respectively. Accordingly, in Europe, Japan, US, the GIL is already employed as bulk power transmission system for response of expansion of cities or for solution of environmental problem. Companies are moving to this progressive technology by means of applying the GIL into constructing new grounding work or replacing part of transmission line. Plenty of companies and research institutes have been studying structural and electrical aspects of GIL with which companies set a plan to apply the technology on-site. The criteria of this technology are almost established through various practical implementations from grounding theories to practical construction. GIL technology accords with satisfaction in demand of industrial renewable energy and eco-environmental technology by reducing ratio of SF6 less than 20% on-site as well as the changes of distance of power plant contribute to the expectation of GIL as new generation power plants such as wind farm requires high capacity long-distance power transmission systems from power generation facilities to load centres. This is because gas-insulated transmission line is new generation technology with its suitability for long-distance power transmission rather than overhead transmission line. Likewise, the understanding of GIL can be recognized to be realisation of future values and furthermore, can be the initial step to coexistence and cooperation with environment, future generation as well [2].

## 1.2. Aims and Objectives

### 1.2.1. Aims

With basis of thorough understanding in power transmission of GIL, suitability will be tested by simulations for long distance bulk power transmission line whether the GIL is appropriate to replace existing transmission lines and existing transmission lines, mainly overhead line, will be considered to be comparison target when environmental and economic comparison discussed. Electrical verification will be primarily conducted as well as subsidiary information will be dealt with such as GIL's design which is composed of three sections in progress report, mixture gas, quality and technical data. The electrical simulation procedure of two software, MATLAB and ATPdraw, will be studied as well as how computational coding is done in each step and what values can be obtained in each probe respectively. Through progress report, comprehensive understanding of simulation based on theory is mainly shown through. For simulation, variables which have already been analysed in literatures or provided by brochure by companies will be used in this report to verify the simulating methods and those results at the same time (however, the reliable data will be chosen for simulation for final report). Supplementary information will be compared based on literature and online information.

### 1.2.2. Objectives

The first 3 objectives shown below is dealt with in each section, 2.1., 2.2. and 2.3. of chapter 2 and the rest will be discussed in conclusion. These objectives are selected to show understanding of GIL and additionally verification of the suitability in GIL to be long distance bulk-power transmission line by simulations.

- Main design features of GIL
- Environmental and Economic impacts of GIL
- Studying simulations of GIL by MATLAB and ATPdraw
- Comprehensive analysis of GIL
- Determination of further research required for final report

## 2. GIL design

### 2.1. Main design features of GIL

#### 2.1.1. $N_2/SF_6$ Gas Mixture

The colourless and odourless $SF_6$ gas can be considered as inert gas chemically, which means the $SF_6$ rarely has a chemical reaction with other molecules as well as thermal stability is outstanding. The $SF_6$ gas is not decomposed before reaching around 500℃ and it has considerably strong dielectric strength under equality electric field which has around 3 times higher dielectric strength than air under the condition of 1 bar. In addition, the dielectric strength of $SF_6$ gas under 3 bar is almost as same as oil.

The $SF_6$ gas has a high arc cancelation performance. The arc under $SF_6$ gas is much stable than in air and show excellent characteristic in breaking high current. This gas has a characteristic of liquefaction so when dealing with it on site the attention on pressure and temperature is required [11].

In first generation of GIL, 100% of $SF_6$ is used to insulate conductor, after that in second generation of GIL mixing gas composed of less than 20% of $SF_6$ and higher than 80% of $N_2$ was used, this 20/80 proportion is chosen for this project and is stabilized variable.

#### 2.1.2. Automated orbital welding and ultrasonic check

The reason why this topic is chosen for main design feature of GIL is that the Automated orbital welding system is considerably related to the quality of GIL and it makes GIL work appropriately. In the first generation of GIL, the hand welding was prevalent, but the demand of automatic welding system highly required because the equal quality of GIL could not be expected for huge kilometres work. The automatic welding system influences in the speed of work as well. The failure of tightness in enclosure result in two failures of GIL in technical and environmental aspect. In regards technical problem, the gas emission to the atmosphere by tightness failure make pressure of the gas low which gives rise to defeated insulating capability of GIL. The $SF_6/N_2$ gas mixture has lower insulating capability than 100% $SF_6$ gas and the disadvantage is compensated by higher pressure. aluminium can be easily corroded when the gas is compounded of moisture as well. With regard to environmental problem $SF_6$ has much higher global-warming potential in comparison to $CO_2$ and this gas is highly restricted by the Kyoto protocol [8].

### 2.1.3. Technical data examples of GIL

| | Siemens | Azz CGIT | Areva | CGIT Westboro, Inc. |
|---|---|---|---|---|
| Nominal Voltage (kV) | 245 to 550 | 420 | 420 | 420 |
| Typical rated current (A) | Up to 4,500 | 4,500 | 4,000 | 3150 |
| Laying method | Underground | Overground | Overground | Underground |
| Gas Mixture | $SF_6$ 20% | $SF_6$ 100% | $SF_6$ 10% | $SF_6$ 100% |
| Gas pressure(bar) | 7 | 4 | 9.3 | 4.8 |
| Conductor diameter(mm) | 180 | 180 | 180 | 127 |
| Conductor Thickness(mm) | 15 | 10 | 11 | 12.7 |
| Enclosure diameter(mm) | ~375 to 522 | 520 | 520 | 371.91 |
| Enclosure Thickness(mm) | - | 10 | 10 | 4.98 |

Table 1. Technical data in company (Park, Jang and Kim, 2008) [10]

As can be seen above, the various models of GIL are employed. In this project, the technical data from the thesis, Evaluation of gas insulated lines(GIL) for long distance HVAC power transfer (Elnaddab, 2014), will be mainly used for power flow simulating in GIL transmission line since the data which company provided over brochure or website tend to be old or have no sufficient data with empty spaces.

## 2.2. Environmental and economic impacts of GIL

### 2.2.1. Environmental impacts of GIL

The development of GIL led to eco-environmental power industry when compared to overhead transmission line. Construction of overhead transmission line effects on nature, life environment. Limitation in selecting site of power plant, generally power plant located far from residential area, causes construction of incalculable length of overhead transmission line. This construction need to be carried out over forest area or the mountain and in this procedure the damage on those place is inevitable. Audible noise around bulk-power overhead transmission line is also one of unavoidable problem and which is called 'hum noise' [5]. Additionally, coronas can bring about audible and radio frequency noise mostly nearby bulk-power overhead transmission lines [4]. The health of residences living around the transmission line should be cared. In article about the relation between EM field and body health, it presents that the EM field influences on our eyes and pineal gland imbalanced (the pineal gland which is one of hormone system manages harmony of hormone action inside human body [3]). On the other hand, GIL can be considered to turn the tables on overhead transmission line's negative effects. The forest and mountain can be preserved by burying transmission line underground as well as the buried GIL does not make any noise since GIL is concealed by soil directly or by tunnel. GIL does not make considerable magnetic field compared to overhead line.

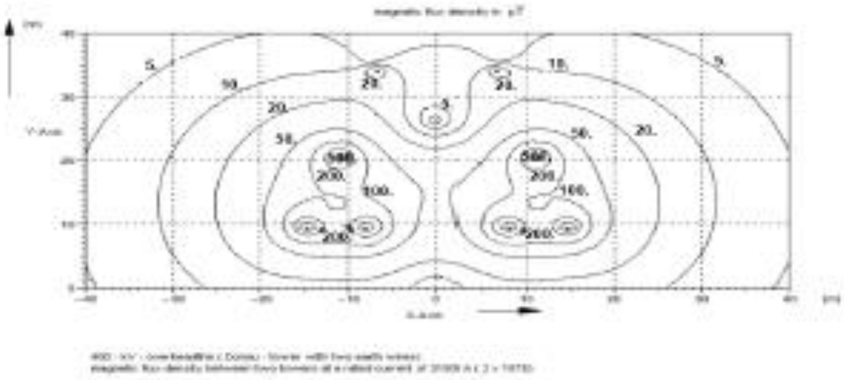

Figure 1. Magnetic flux calculated overhead line [6]

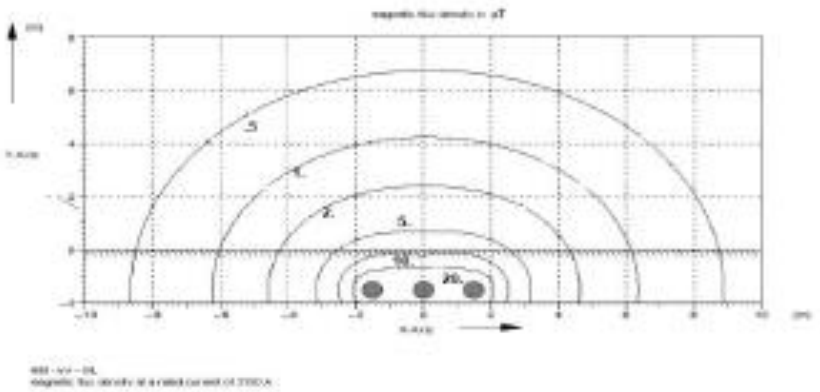

Figure 2. Magnetic flux calculated GIL [6]

The diagrams above show that the magnetic field of overhead line 8 times stronger than of GIL. One concern of disadvantage on environmental of GIL is its insulating media, $SF_6$. The worry about it has been reduced as gas ratio changes falling down to less than 20% but still anxiety stays in case of failure in tightness of enclosure. The alternative gas, $CF_3I$, of $SF_6$ has introduced but the alternative gas will not be handled in this project since the $SF_6/N_2$ gas mixture will be considered to be stabilised variable [8].

### 2.2.2. Economic impacts of GIL

One of main impediment to be being prevalent in use of GIL is its low competitive price. $SF_6$ gas is an artificial gas and it is expensive. although the less the ratio of $SF_6$ in gas mixture is, the higher the competitive price has, Undergrounding GIL technology is still expensive.

| | Capital build cost – per km | Total Life-time cost (build and operation and maintenance) – per km |
|---|---|---|
| Overhead | £1.6m | £4.0m |
| Underground | £16.7m | £18.9m |
| Cost Difference | £15.1m | £14.9m |
| Ratio | Approx. 10:1 | Approx. 5:1 |

Table 2. Cost of overhead and underground line [12]. National Grid report (2012)

The table above indicates the difference of cost between overhead transmission line and underground transmission line. When the GIL is considered instead of underground transmission line, the cost will significantly increase because the $SF_6$ gas and aluminium is high-priced. Furthermore, if tunnel is needed to set up, the cost will remarkably go up for which £8.913 M per km [8] of additional cost imposed. Nevertheless, the high initial investment of GIL is compensated by its long-life time and maintenance cost is not required in accordance with literature. The lifespan of insulator of overhead transmission line is about 40 years even though pylons will last about 80years. It means the insulator has to be refurbished at least once before its lifespan, but GIL has 50 years lifespan, and which results in reduction of maintenance cost.

## 2.3. Long-distance power transmission of GIL by simulating

### 2.3.1. MATLAB simulation

To figure out the patterns of graph in receive voltage, current, real power and reactive power. 420kVrms is used for this simulation with power factor = 0.8.

| | |
|---|---|
| Resistance per phase(mΩ/Km), r | 8.6 |
| Inductance per phase(mH/Km), l | 0.204 |
| Capacitance per phase (uF/Km), C | 0.0545 |
| Longitudinal impedance (m Ω /km), Z=r+jωl | 8.616+j64 |
| Shunt admittance (mS/km), Y=g+jωc | 0+j0.017 |
| Characteristic Impedance (Ω), $Z_0=\sqrt{Z\times Y}$ | 61.64-j4.1 |
| Propagation Constant (1/km), $\gamma=\sqrt{Z*Y}$ | 0.0001+j0.001 |
| Surge Impedance Loading at 420kV(MVA), SIL=$(420kV)^2/\lvert Z_0\rvert$ | 2893.6 |

Table 3 GIL parameters [8]

For plotting diagrams, the variables in table 3 is used and these data come from a thesis by Elnaddab K. (2014). The data above match in variables ABCD below.

$$V_R = AV_S - BI_S \quad (1)$$

$$I_R = DI_S - CV_S \quad (2)$$

$$P_R = |V_R||I_R|\cos(\theta_V - \theta_I) \quad (3)$$

$$Q_R = |V_R||I_R|\sin(\theta_V - \theta_I) \quad (4)$$

the equations, (1) to (4), are used to plot the graphs 1 to 4 respectively.

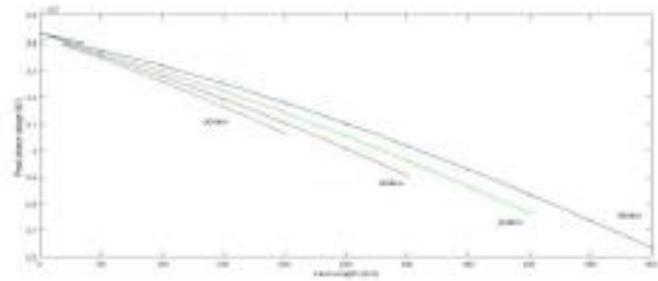

Figure 3 (a) Peak phase voltage by length with MATLAB

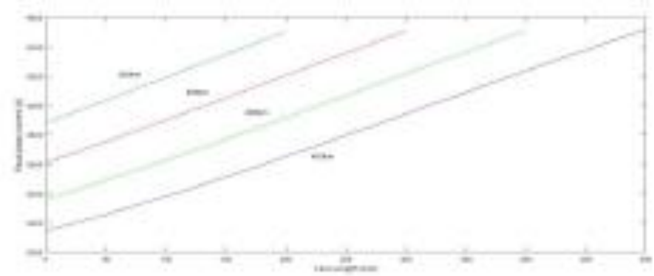

Figure 3 (b) Peak phase current by length with MATLAB

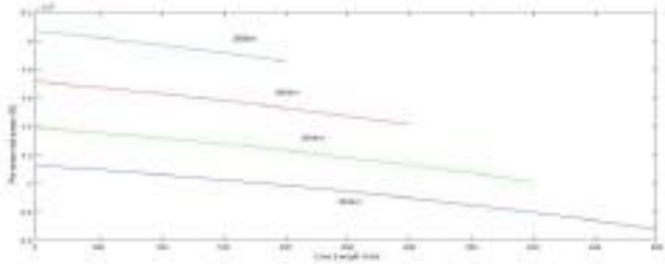

Figure 3 (c) Real power per phase by length with MATLAB

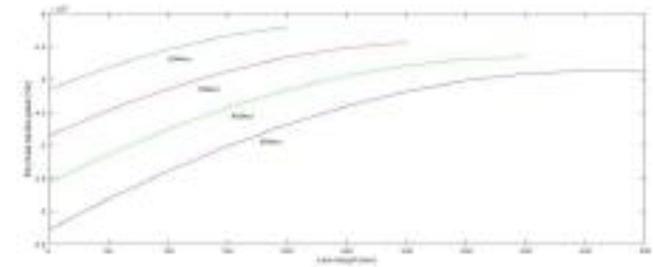

Figure 3 (d) Reactive power per phase by length with MATLAB

School of Electrical and Electronic Engineering Page 8

### 2.3.2. ATPdraw simulation

| Line length (Km) | $Z_{Load}\ (\Omega)$ |
|---|---|
| 200 | 55+j39.9 |
| 300 | 52+j38 |
| 400 | 49.35+j36.3 |
| 500 | 47+j34.54 |

Table 4 Load impedances by line length operating at cos(θ) = 0.8 [9]

Impedances of load for each line length simulation are indicated over Table 4 to attain thermal current limit 3180A as well as power factor is 0.8 and these data are filled out into the load at the end of the transmission line on Figure 3. Sending voltage, $V_s$, is $420\angle 0^{\circ} kV_{rms}$ so 342.93kV of voltage per phase is rated at the first voltage probe on Figure 3, and 4497.2A is observed on the last current probe over all distance simulation. Impedance on transmission line is 0.43+j3.2 per 50km calculated from Table 3.

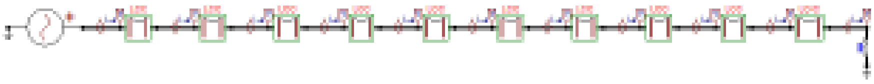

Figure 4 GIL simulation model with ATPdraw

With materials above, Table 4, Figure 3 and basic premises, the 4 graphs can be plotted. Results authentication will be carried out with earlier plotted graph on reference, Elnaddab, K. (2014).

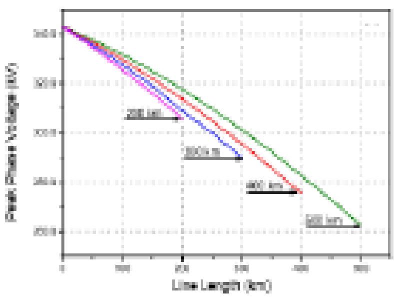


Figure 5 (a) Peak phase voltage drop by length [8]

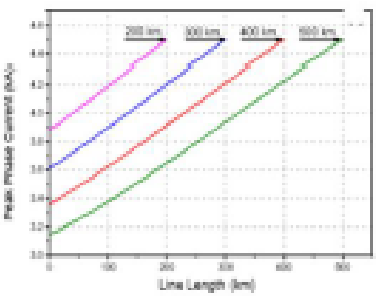


Figure 5 (b) Peak phase current rise by length [8]

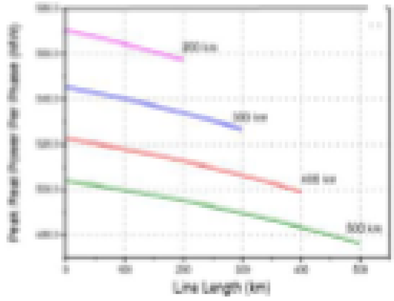


Figure 5 (c) Peak real power drop by length [8]

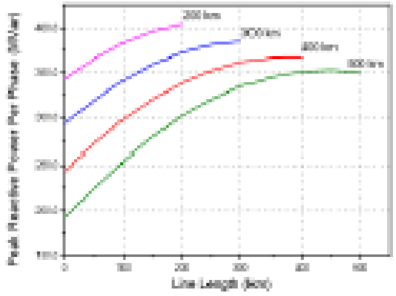


Figure 5 (d) Peak reactive power rise by length [8]

# 3. Conclusion

## 3.1. Comprehensive analysis of GIL

Effective value of GIL can be recognised to be substantial with its eco-environmental and economic potential. GIL has not yet reached the end of its technological progress such as researching of alternative gas. Moreover, GIL improves the quality of human life by reducing noise, preserving natural view and rescuing from strong electromagnetic field. Even though GIL's initial installation price is a concern, many advantages compensate its drawbacks with its low maintenance price for next 50 years infrastructure. By simulation, effectiveness of GIL getting higher is proven as longer distance of transmission line installed.

## 3.2. Determination of further research required for final report

Reliable data collection must be conducted by taking more time in browsing information about GIL as well as data refinement. sufficient data are over online, which is easily approachable but substantive on-site data is deficient, or narrowly provided, such as technical data of GIL from brochure by companies. With sufficient and respectable data, simulation need to be repeated in many times to make it thoroughly writer's work. Already introduced MATLAB code is used to analyse long distance transmission of GIL in 2.3.1. on progress report but another way to express and write code of research is required with ATPdraw as well. Furthermore, exhaustive research on literature will lead to better essay on final report by Looking at GIL from various angles. Divers research will be introduced to figure out GIL from basic design criteria to its quality, which is expected reader to understand systematically.

## 4. References


[1] Transmission-line.net. (2017). *HISTORY OF GAS INSULATED TRANSMISSION LINE INFORMATION*. [online] Available at: http://www.transmission-line.net/2012/02/history-of-gas-insulated-transmission.html [Accessed 26 Oct. 2017].

[2] Renewableenergyworld.com. (2017). *Why is renewable energy important?* [online] Available at: http://www.renewableenergyworld.com/index/tech/why-renewable-energy.html [Accessed 26 Oct. 2017].

[3] Consumerhealth.org. (2017). *Consumer Health Articles: THE NEGATIVE EFFECTS OF ELECTROMAGNETIC FIELDS*. [online] Available at: http://www.consumerhealth.org/articles/display.cfm?ID=19990303201129 [Accessed 26 Oct. 2017].

[4] En.wikipedia.org. (2017). *Corona discharge*. [online] Available at: https://en.wikipedia.org/wiki/Corona_discharge [Accessed 26 Oct. 2017].

[5] Li, Q., Shuttleworth, R., Zhang, G., Dupere, I. and Rowland, S. (2013). Acoustic noise evaluation for overhead line conductors. *2013 IEEE Electrical Insulation Conference (EIC)*.

[6] CGIT Bus Systems Problem solving solutions. (2005).

[7] Siemens AG (n.d.). Experience with 2nd Generation Gas-Insulated Transmission Lines GIL. 91052 Erlangen Germany.

[8] Elnaddab, K. (2014). Evaluation of Gas Insulated Lines (GIL) for Long Distance HVAC Power Transfer. Doctor of Philosophy. School of Engineering Cardiff University.

[9] Elnaddab, K., Haddad, A. and Griffiths, H. (2017). The Transmission Characteristics of Gas Insulated Lines (GIL) Over Long Distance. UK.

[10] Park, H., Jang, T. and Kim, J. (2008). A Study on the GIL Modeling by ATP/Draw(EMTP). The Korean Institute of Electrical Engineers, [online] pp.307-308 (2 pages). Available at: http://www.dbpia.co.kr/Article/NODE01336679 [Accessed 26 Oct. 2017].

[11] Kepco.pe.kr. (2017). [online] Available at: http://kepco.pe.kr/technote/read.cgi?board=bal03&y_number=85&nnew=2&ck attempt=2 [Accessed 26 Oct. 2017].

[12] National Grid (2012). *Electricity Transmission Cost Study: How does the independent report compare to National Grid's view?* UK: The Institution of Engineering and Technology and Parsons Brinckerhoff.

## 5. Appendix – Project plan and Risk assessment

| Project plan | Duration | Start Week | Finish Week |
|---|---|---|---|
| **Review of literature** | | | |
| Academic materials review | 32 Weeks | 4th Week of Sep | 4th Week of Apr |
| Software simulating | 21 Weeks | 3rd Week of Oct | 1st Week of Apr |
| **Progress report** | | | |
| Gantt chart | 2 Weeks | 2nd Week of Oct | 4th Week of Oct |
| Academic malpractice | 1day | 3rd Week of Oct | 3rd Week of Oct |
| Risk accessment | 1 day | 4th Week of Oct | 4th Week of Oct |
| Writing report | 3 Weeks | 2nd Week of Oct | 4th Week of Oct |
| **The final report** | | | |
| Writing report | 12 Weeks | 1st Week of Feb | 4th Weeks of Apr |
| **Oral examination and poster** | | | |
| Practice presentation skills | 2 Weeks | 1st Week of May | 2nd Week of May |
| Making poster | 2Weeks | 1st Week of May | 2nd Week of May |

Semester 1 Semester 2

Sep Oct Nov Dec Jan Feb Mar Apr May



MANCHESTER 1824
The University of Manchester

## General Risk Assessment Form

| Date: 26th Oct 2017 | Assessed by: Seunghwan Kim | Checked by: | Location: Mainly room | Assessment ref no | Review date: Less than 1 year |
|---|---|---|---|---|---|

**Task / premises: review of literatures, simulation with software, calculation by hand, searching online.**

| Activity | Hazard | Who might be harmed and how | Existing measures to control risk | Risk rating | Result |
|---|---|---|---|---|---|
| Coding MATLAB | Migraine | Student | Taking a rest every 50 mins and feeling free when coding | Low | T |
| Googling | decreased visual acuity | Student | Using computer under bright lighting | Low | T |
| Calculation by hand | Damage to pencil or paper | Student or nearby | Being careful when handling paper or pencil | Medium | T |
| Review of literatures | haemorrhoid | student | Stretching body every 50 mins | Medium | T |
| Using unfamiliar software - ATPdraw | Failure in simulation | student | Learning essential practical skills. | Medium | T |
| Writing report | Influenza | student | Refraining from smoking, drinking tea and being warm when reporting | High | T |
| Presentation | Tension type headache | student | Relaxing and enough preparation before presentation | Low | T |

## 9.2. Appendix 2 – Results by MATLAB calculation for GIL

i. MATLAB calculation results for electrical power transfer characteristics regarding line length

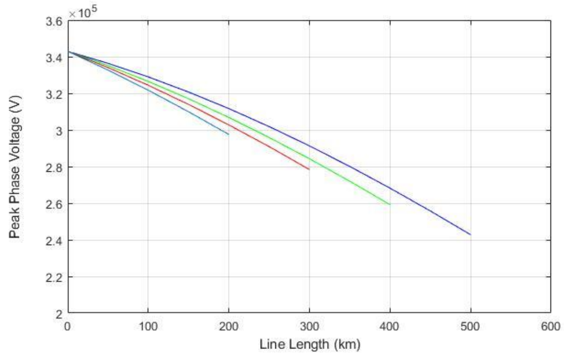


(a) Voltage Drop Profiles

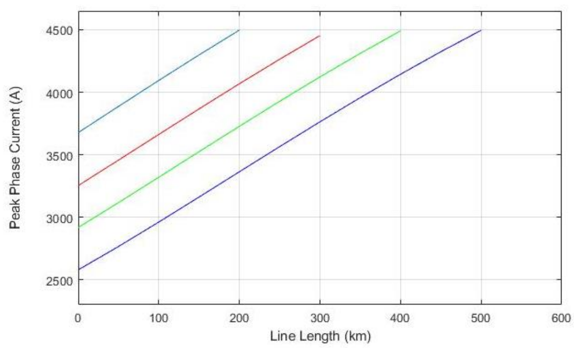


(b) Current Rise Profiles

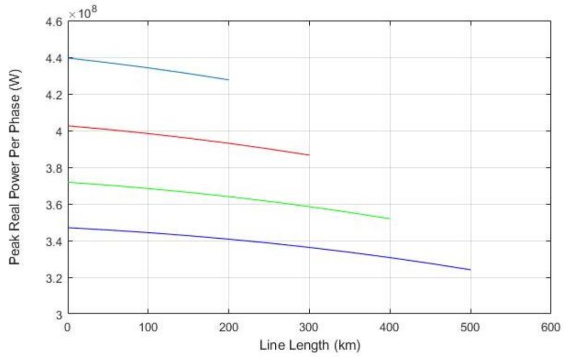


(c) Real Power Losses Profiles

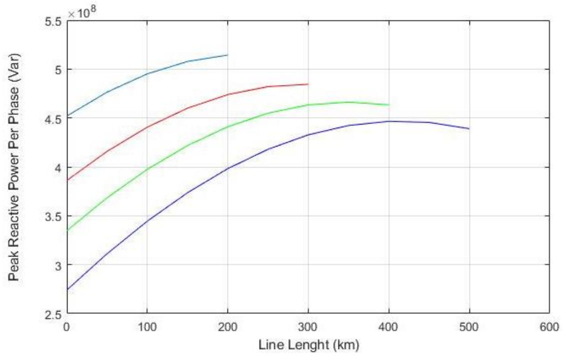


(d) Reactive Power Gain Profiles

## ii. Sending end current set for MATLAB calculation

| Line Length(km) | Sending End Current |
|---|---|
| 200 | $2579\angle 38.3°$ |
| 300 | $2918\angle 42°$ |
| 400 | $3253\angle 43.8°$ |
| 500 | $3677\angle 45.8°$ |

### iii. MATLAB code for calculation, reproduced from Elnaddab. K. PhD thesis (2014)[2]

```
- A= 3677
- B = 45.8
- H= A*sin(B*pi/180)
- O=A*cos(B*pi/180)
-
- A1= 3253
- B1 = 43.8
- H1= A1*sin(B1*pi/180)
- O1=A1*cos(B1*pi/180)
-
- A2= 2918
- B2 = 42
- H2= A2*sin(B2*pi/180)
- O2=A2*cos(B2*pi/180)
-
- A3= 2579
- B3 = 38.3
- H3= A3*sin(B3*pi/180)
- O3=A3*cos(B3*pi/180)
-
- R= 7.097e-3
- l=2.158e-4
- c=54.3e-9
- f=50
- I=j*2*pi*f*l
- z=R+I
- y=j*2*pi*f*c
- Zc=sqrt(z/y)
- ga=sqrt(z*y)
- L1=[0:50:500]
- L2=[0:50:400]
- L3=[0:50:300]
- L4=[0:50:200]
- B1=Zc.*sinh(L1.*ga);
- B2=Zc.*sinh(L2.*ga);
- B3=Zc.*sinh(L3.*ga);
- B4=Zc.*sinh(L4.*ga);
- A1=cosh(L1.*ga);
- A2=cosh(L2.*ga);
- A3=cosh(L3.*ga);
- A4=cosh(L4.*ga);
- C1=(sinh(L1.*ga))./Zc
- C2=(sinh(L2.*ga))./Zc
- C3=(sinh(L3.*ga))./Zc
- C4=(sinh(L4.*ga))./Zc
- Vs=complex(342928.6,0)
- Is1=complex(O3,-H3)
- Is2=complex(O2,-H2)
- Is3=complex(O1,-H1)
- Is4=complex(O,-H)
```

- Vr1=(A1.*Vs)-(B1.*Is1);
- Vr2=(A2.*Vs)-(B2.*Is2);
- Vr3=(A3.*Vs)-(B3.*Is3);
- Vr4=(A4.*Vs)-(B4.*Is4);
- V1=abs(Vr1);
- V2=abs(Vr2);
- V3=abs(Vr3);
- V4=abs(Vr4);
- plot(L1,V1,'b',L2,V2,'g',L3,V3,'r',L4,V4)
- Ir1=(A1.*Is1)-(C1.*Vs)
- Ir2=(A2.*Is2)-(C2.*Vs)
- Ir3=(A3.*Is3)-(C3.*Vs)
- Ir4=(A4.*Is4)-(C4.*Vs)
- I1=abs(Ir1)
- I2=abs(Ir2)
- I3=abs(Ir3)
- I4=abs(Ir4)
- plot(L1,I1,'b',L2,I2,'g',L3,I3,'r',L4,I4)
- thV1=angle(Vr1)
- thV2=angle(Vr2)
- thV3=angle(Vr3)
- thV4=angle(Vr4)
- thI1=angle(Ir1)
- thI2=angle(Ir2)
- thI3=angle(Ir3)
- thI4=angle(Ir4)
- V1=V1./sqrt(2)
- V2=V2./sqrt(2)
- V3=V3./sqrt(2)
- V4=V4./sqrt(2)
- I1=I1./sqrt(2)
- I2=I2./sqrt(2)
- I3=I3./sqrt(2)
- I4=I4./sqrt(2)
- P1=(V1.*I1).*cos(thV1-thI1)
- P2=(V2.*I2).*cos(thV2-thI2)
- P3=(V3.*I3).*cos(thV3-thI3)
- P4=(V4.*I4).*cos(thV4-thI4)
- plot(L1,P1,'b',L2,P2,'g',L3,P3,'r',L4,P4)
- Q1=(V1.*I1).*sin(thV1-thI1)
- Q2=(V2.*I2).*sin(thV2-thI2)
- Q3=(V3.*I3).*sin(thV3-thI3)
- Q4=(V4.*I4).*sin(thV4-thI4)
- plot(L1,Q1,'b',L2,Q2,'g',L3,Q3,'r',L4,Q4)